Euclid detectability of pair instability supernovae in binary population synthesis model consistent with merging binary black holes

Komaba colloquium, June 2 2022

Ataru Tanikawa

Tanikawa, Moriya, Tominaga, Yoshida (2022, arXiv:2204.09402)

Gravitational wave

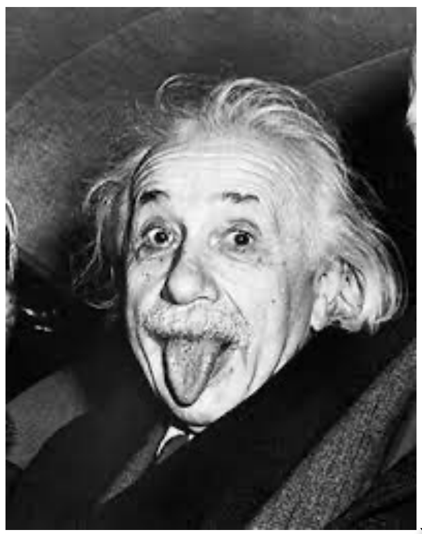

Einstein's field equations

$$G_{\mu\nu} \equiv R_{\mu\nu} - \frac{1}{2} R\, g_{\mu\nu} = \frac{8\pi G}{c^4} T_{\mu\nu}$$

Predicted 1916

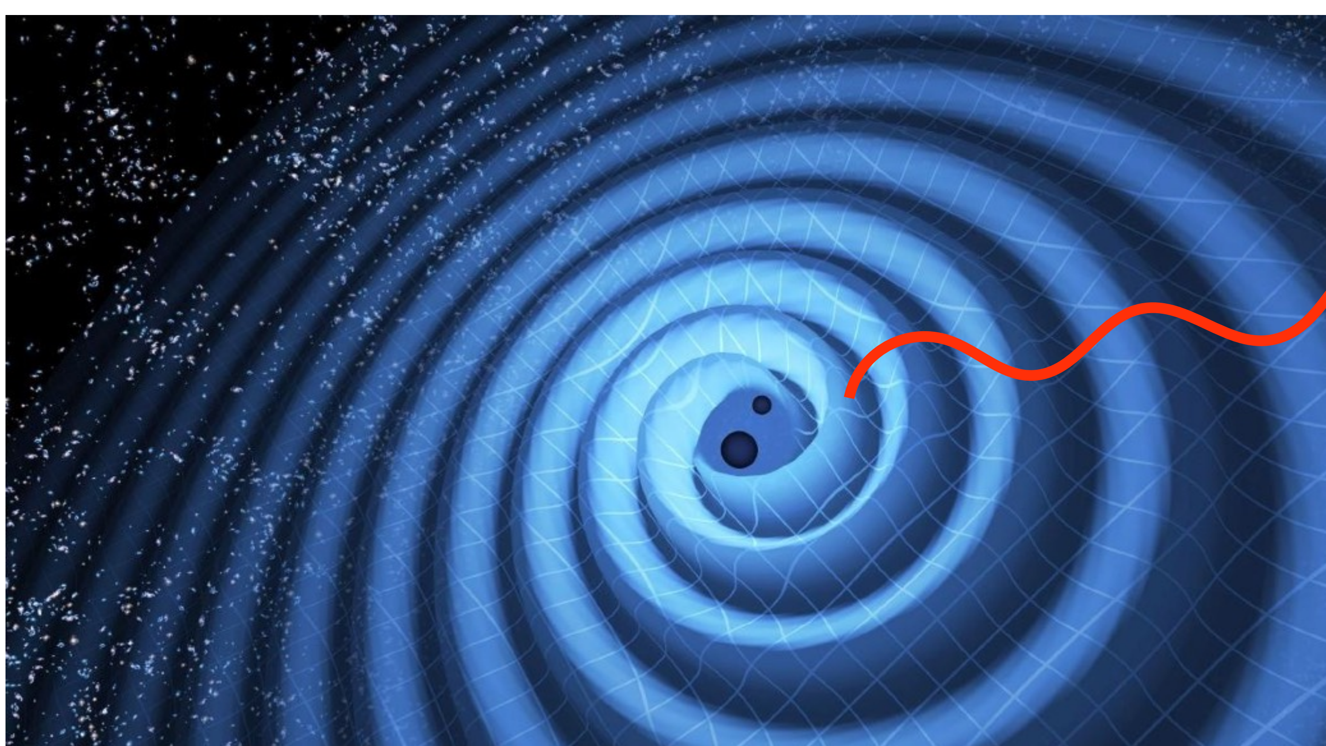

Indirect evidence by Hulse-Taylor binary (1975)

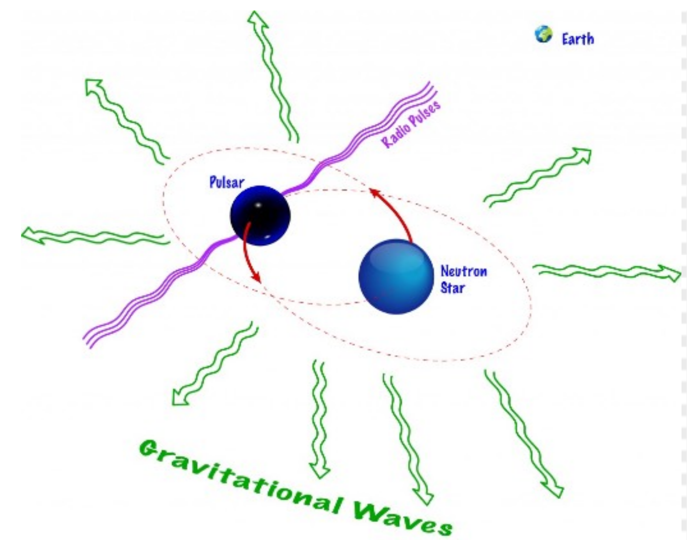

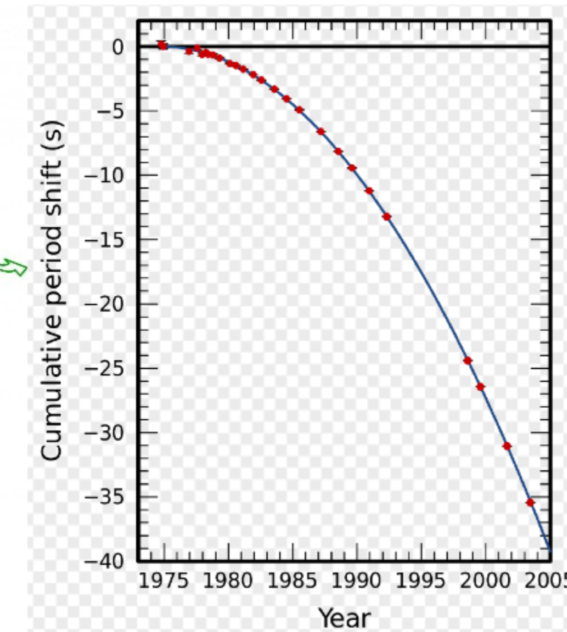

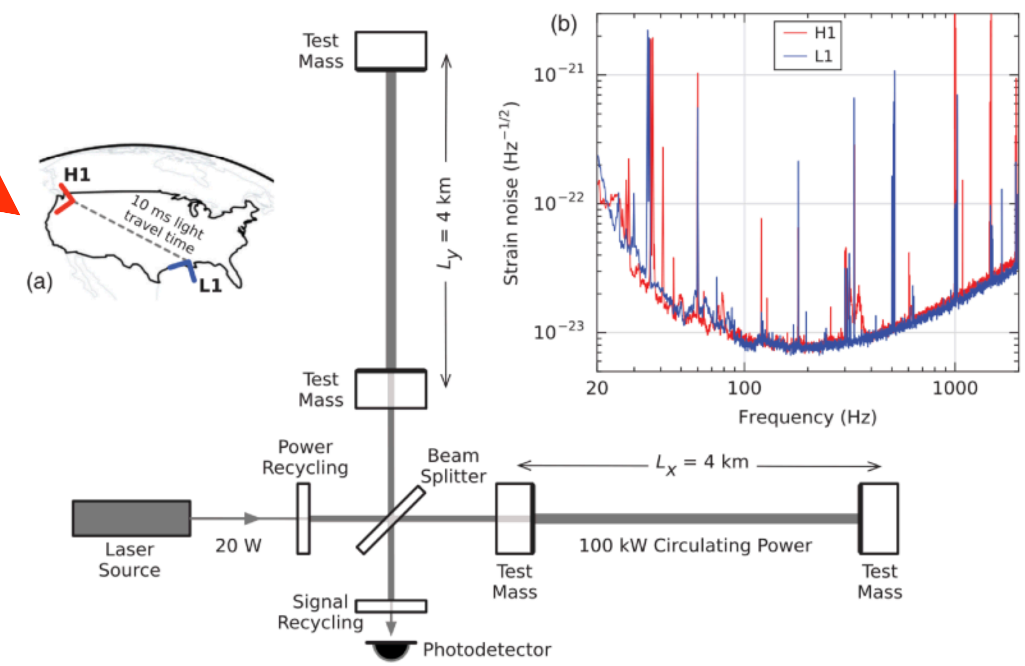

Direct observation by LIGO (2015)

Binary black holes

The first detection 2015/09/14 (GW150914)

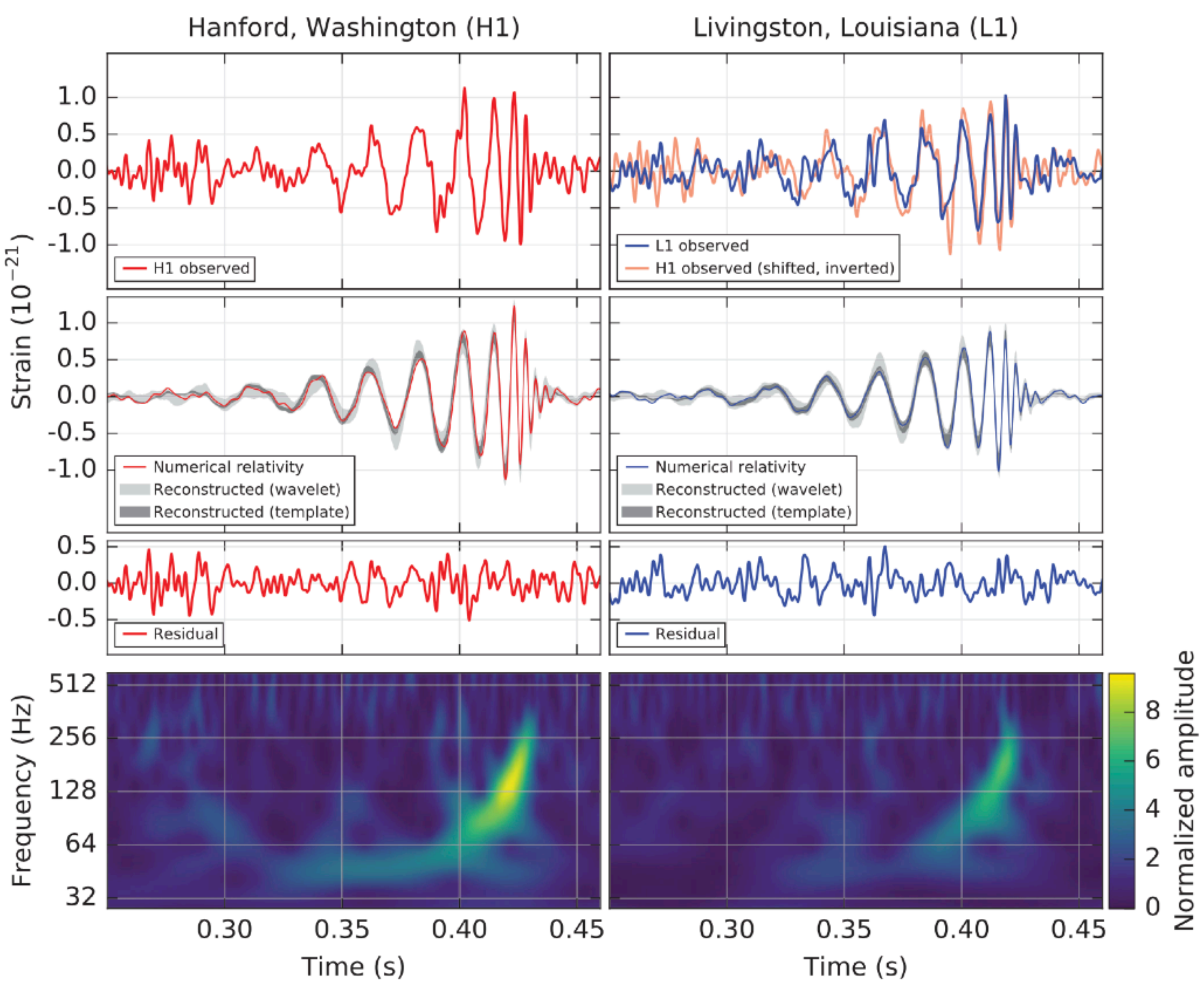

$\sim 30M_{\odot}$ BH

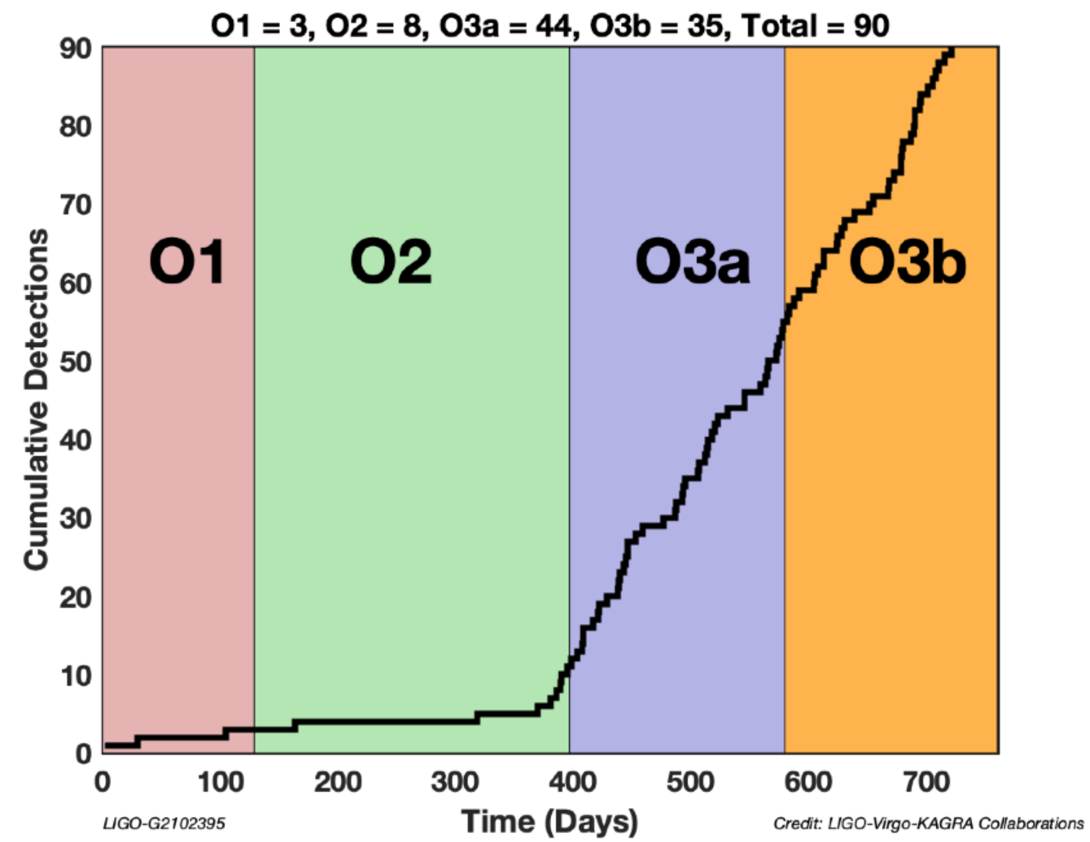

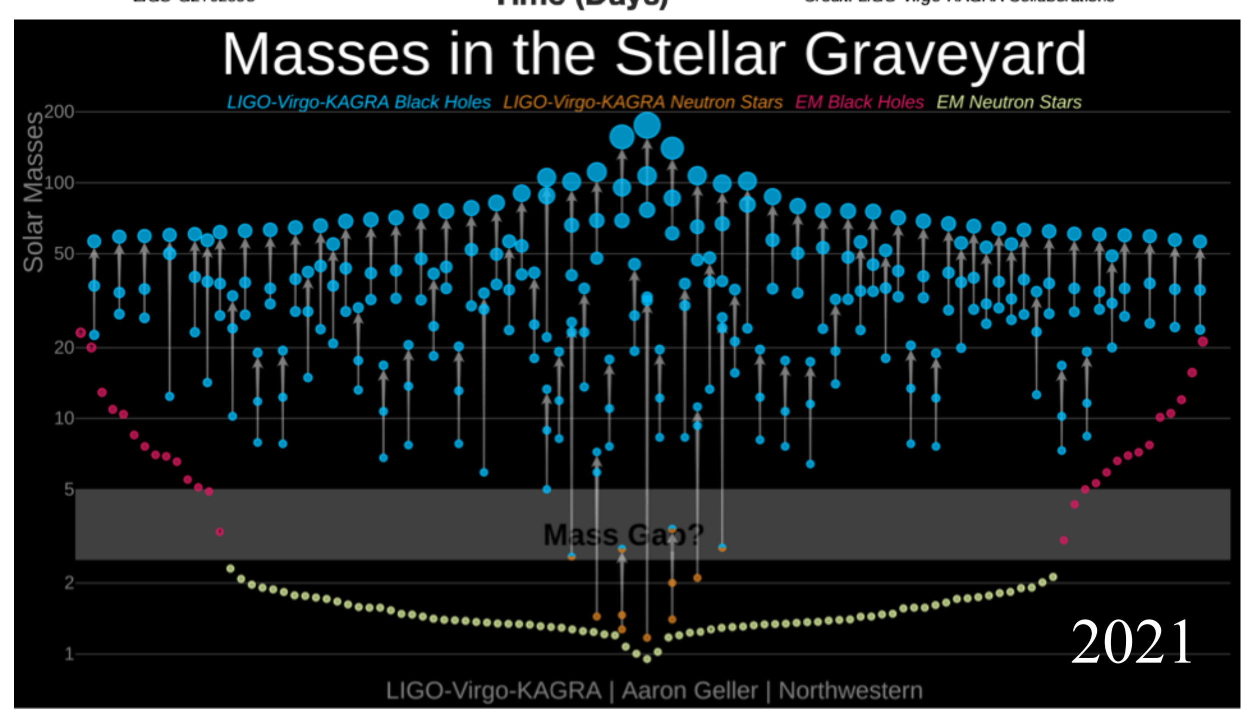

Origin of binary black holes

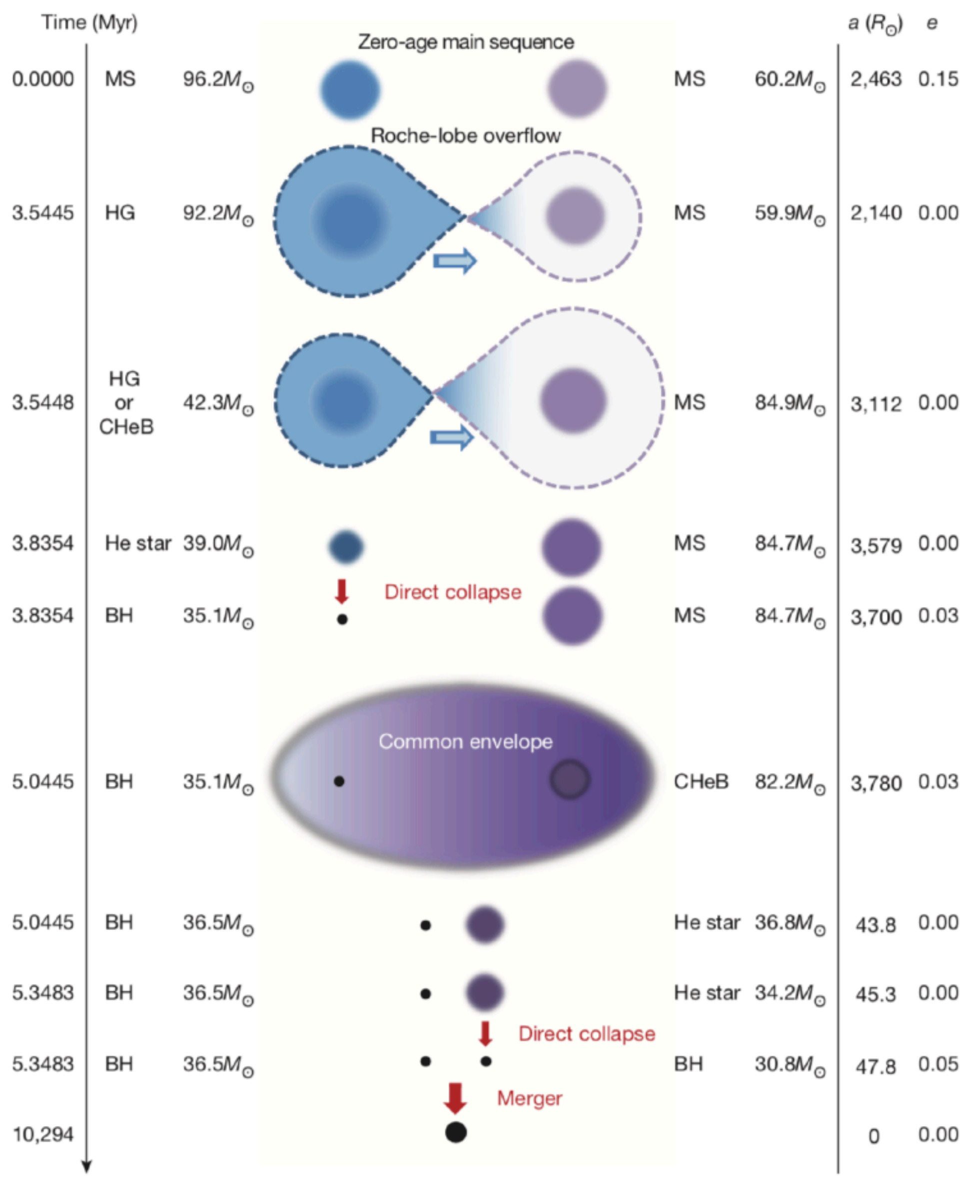

Belczynski et al.; Eldridge et al.; Giacobbo et al.; Kinugawa et al.; Kruckow et al.; Stevenson et al.; Tanikawa et al.;

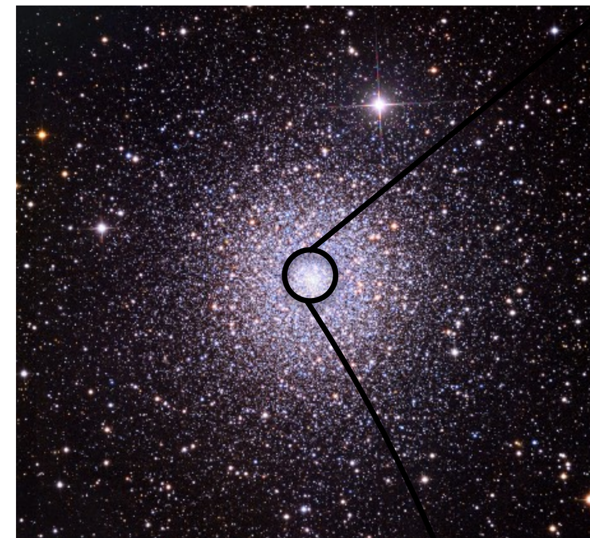

- Open clusters
- Globular clusters (Rodrigeuz et al.; Askar et al.; Wang et al.)
- AGN disk (Tagawa et al.)

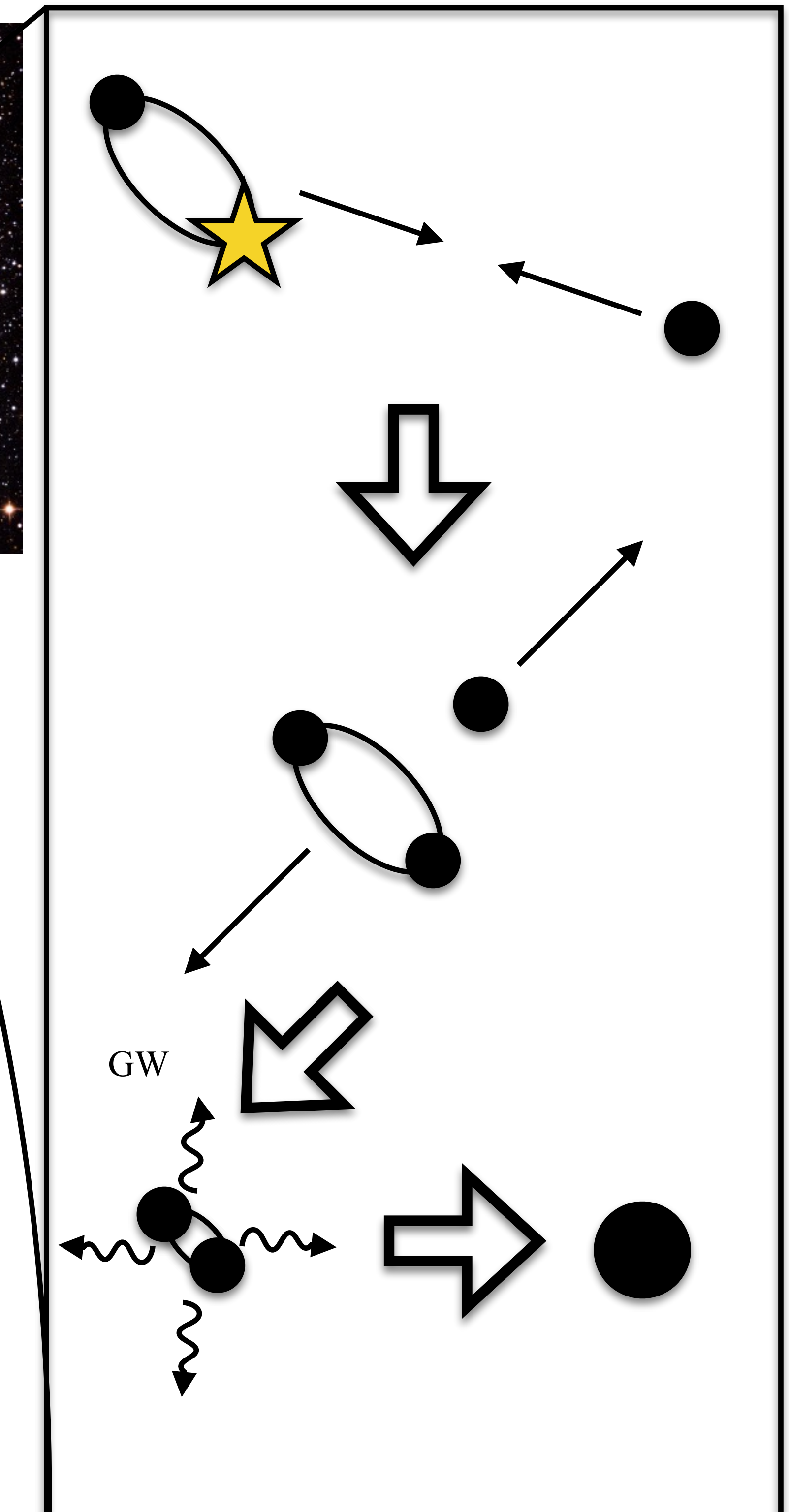

Importance of their origin(s)

- Objects most frequently discovered by GW observations
- Probes for astronomical objects
  - Binary: star formation history, IMF, binary initial condition, stellar evolution, core-collapse supernova, pair instability supernova, supernova kick, etc.
  - Cluster: cluster formation history, cluster initial condition, current dynamical state, etc.
  - Primordial BH: early universe, dark matter, etc.

Localization

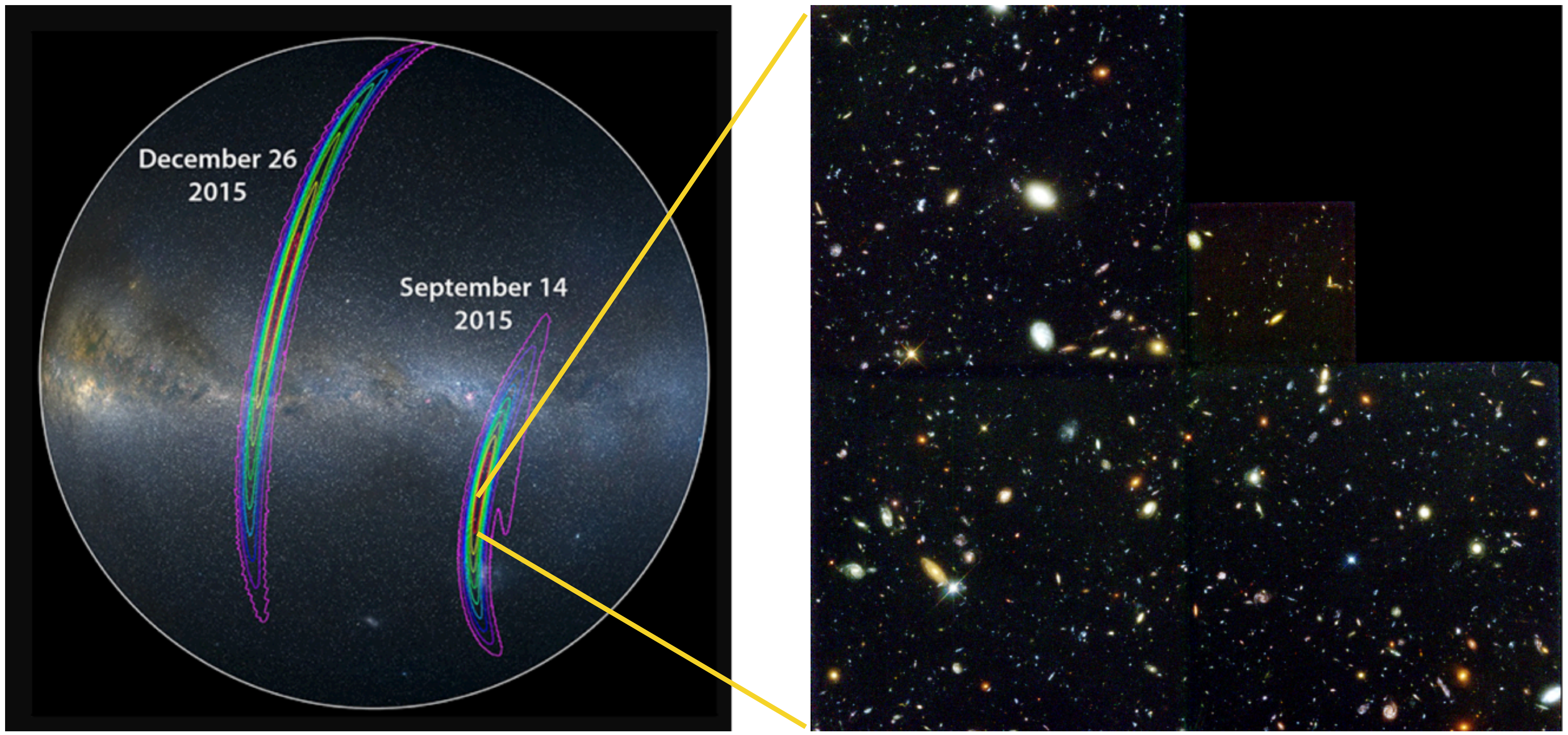

Binary black hole

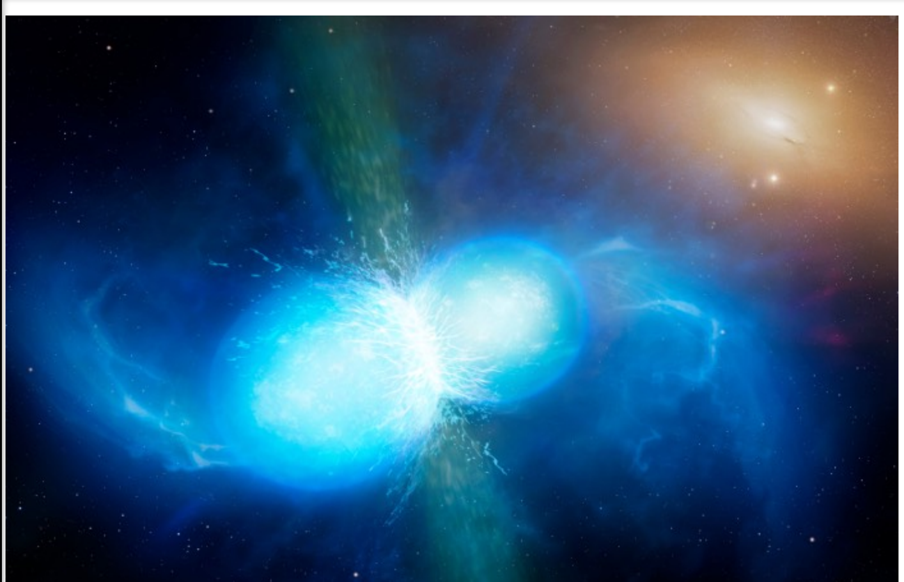

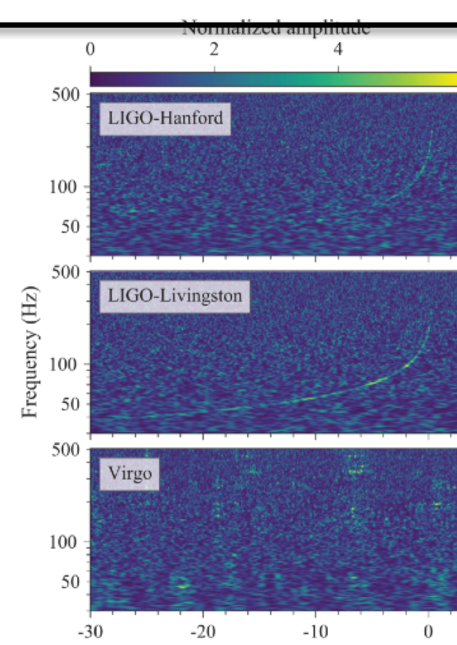

Binary neutron star

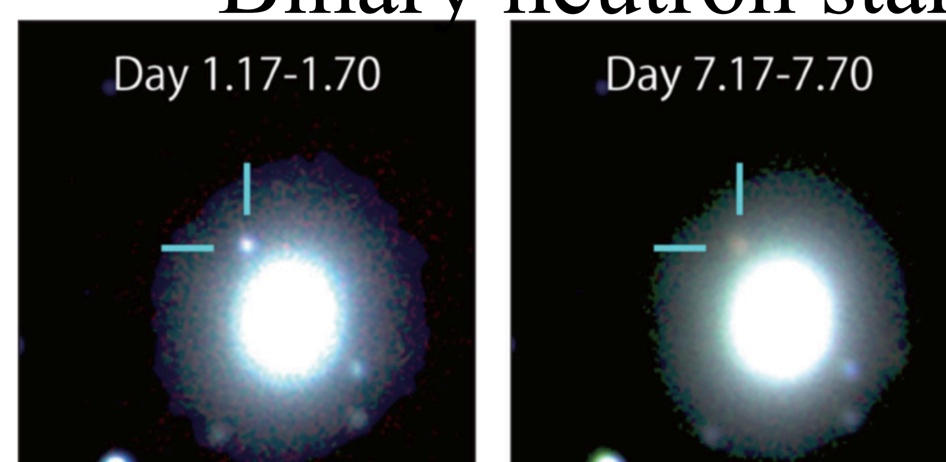

Black hole mass

GW150914 (Abbott et al. 2016)

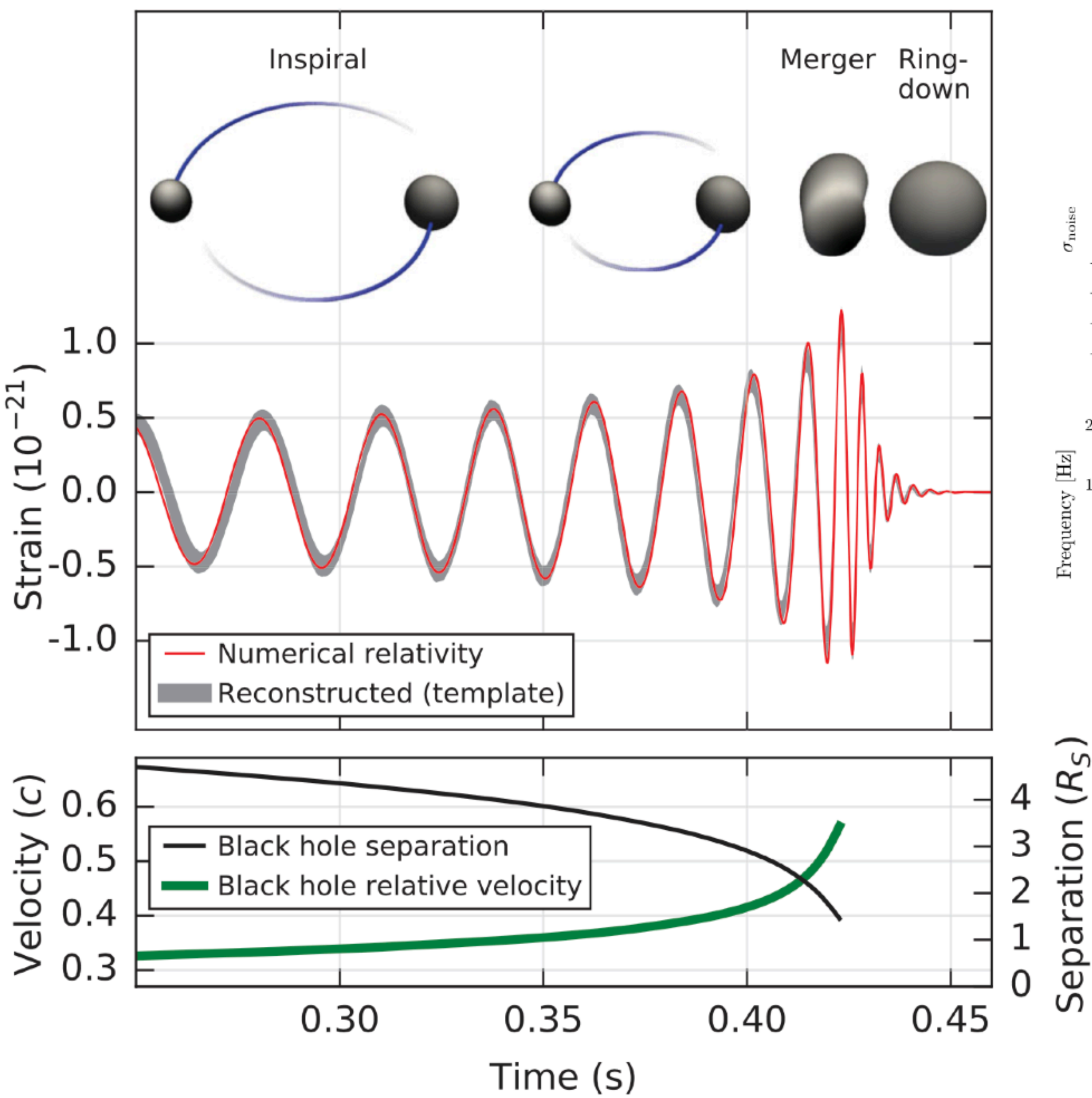

GW190521 (Abbott et al. 2020)

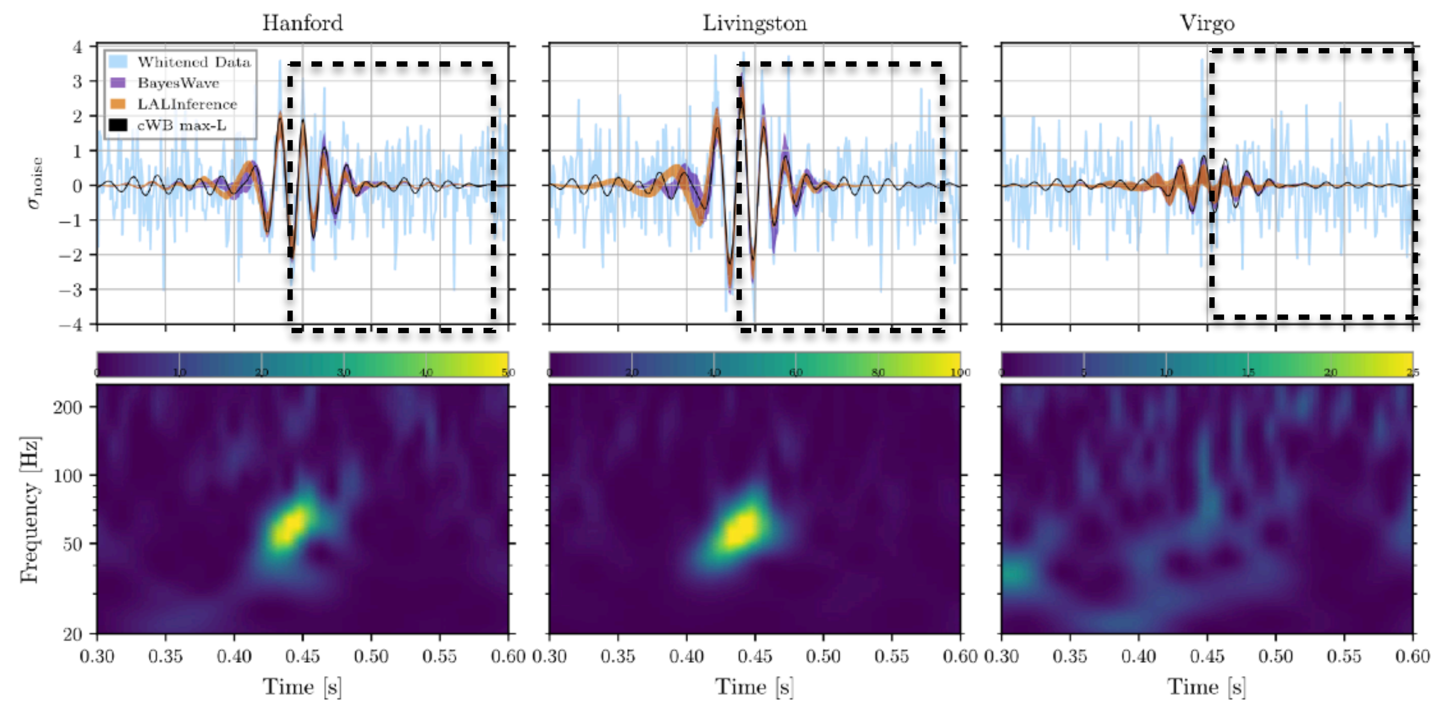

- frequency: $\sim$ 66Hz
- Damping time: $\sim$ 19ms

- Redshifted mass: $\sim 252 M_\odot$
- Source mass: $\sim 142 M_\odot$

$$\mathcal{M} = \frac{(m_1 m_2)^{3/5}}{(m_1 + m_2)^{1/5}} = \frac{c^3}{G}\left[\frac{5}{96}\pi^{-8/3} f^{-11/3} \dot{f}\right]^{3/5}$$

Pair instability supernovae

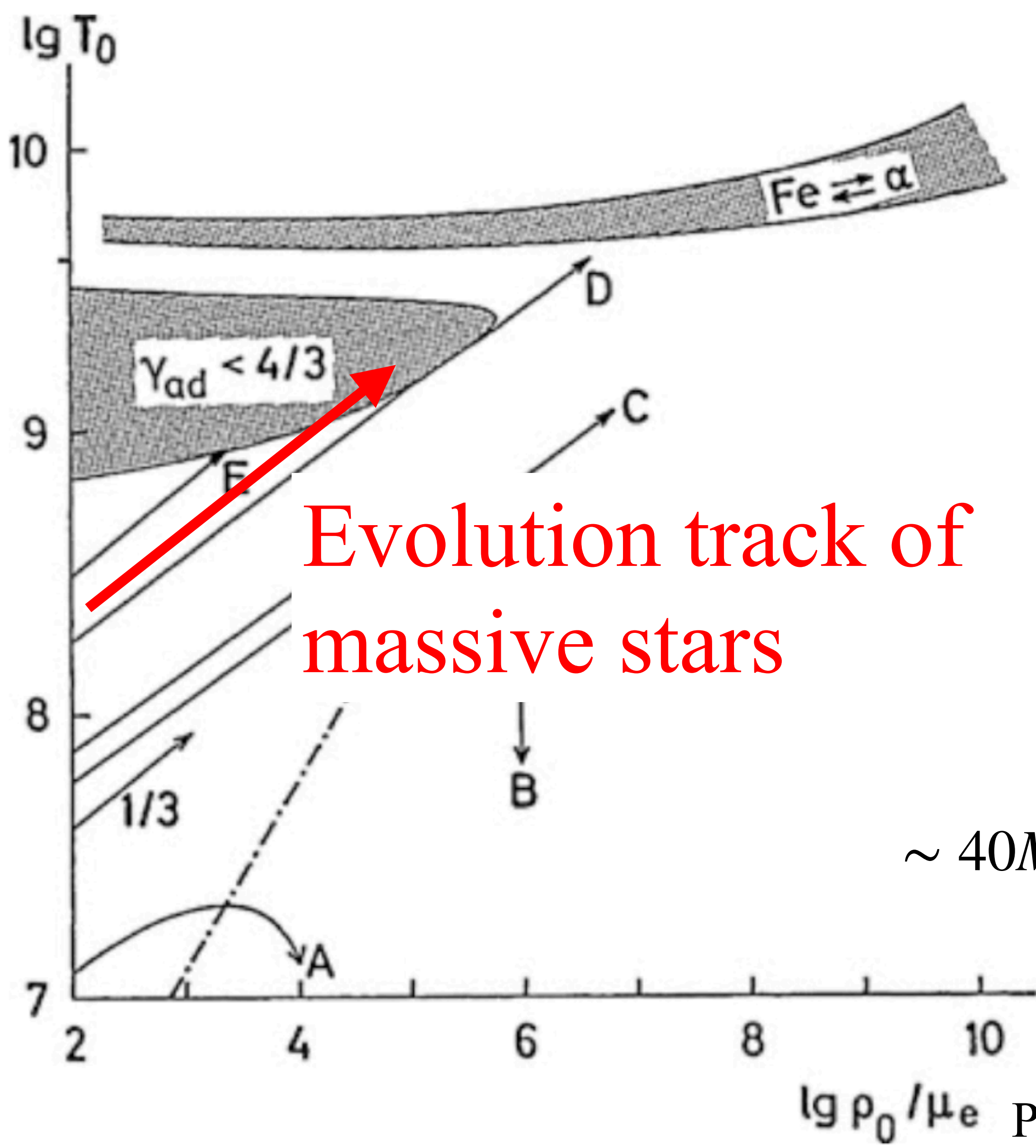

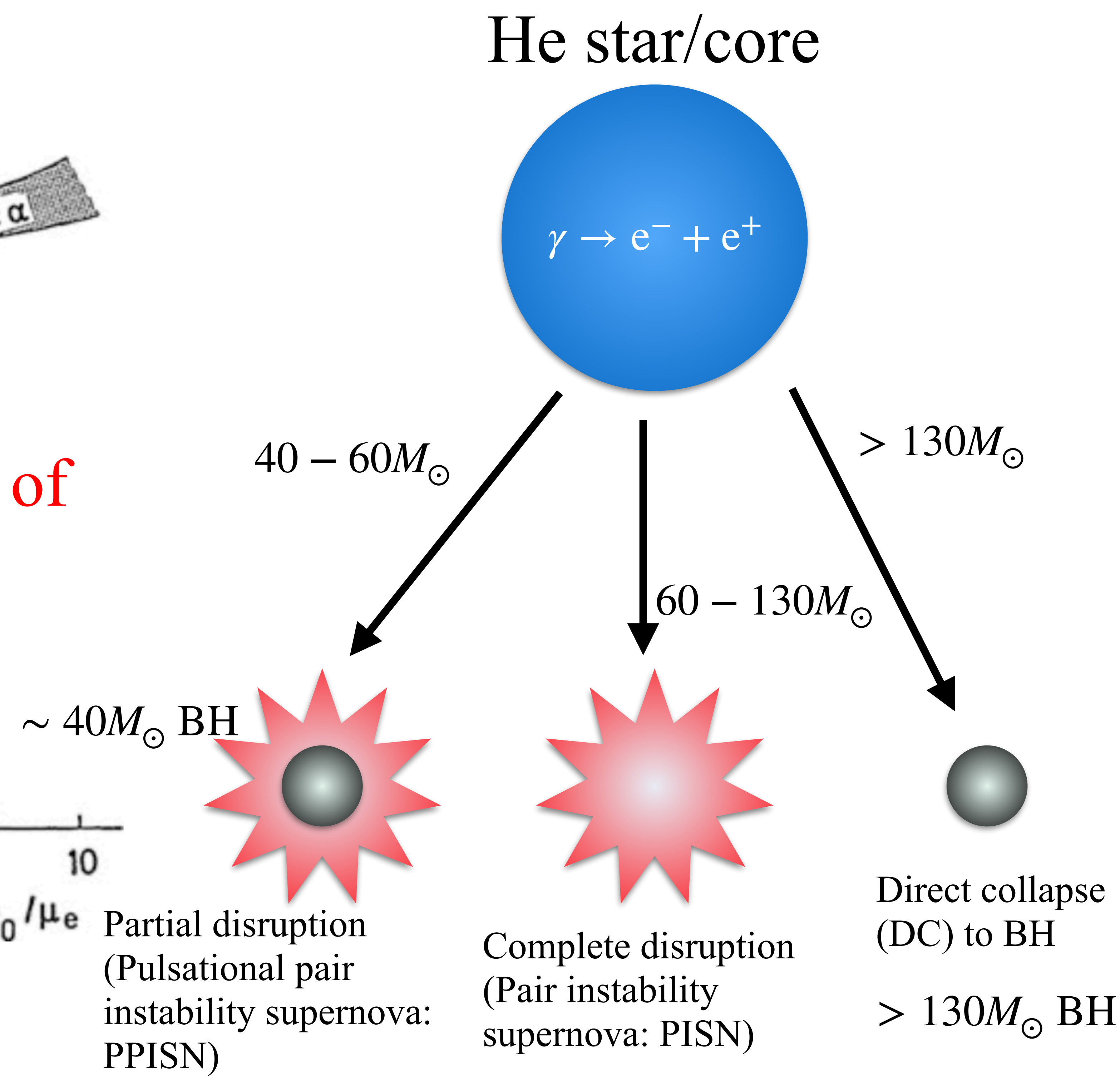

Mass gap between $40 - 130 M_\odot$

Pair instability mass gap

$0.01 Z_{\odot}$

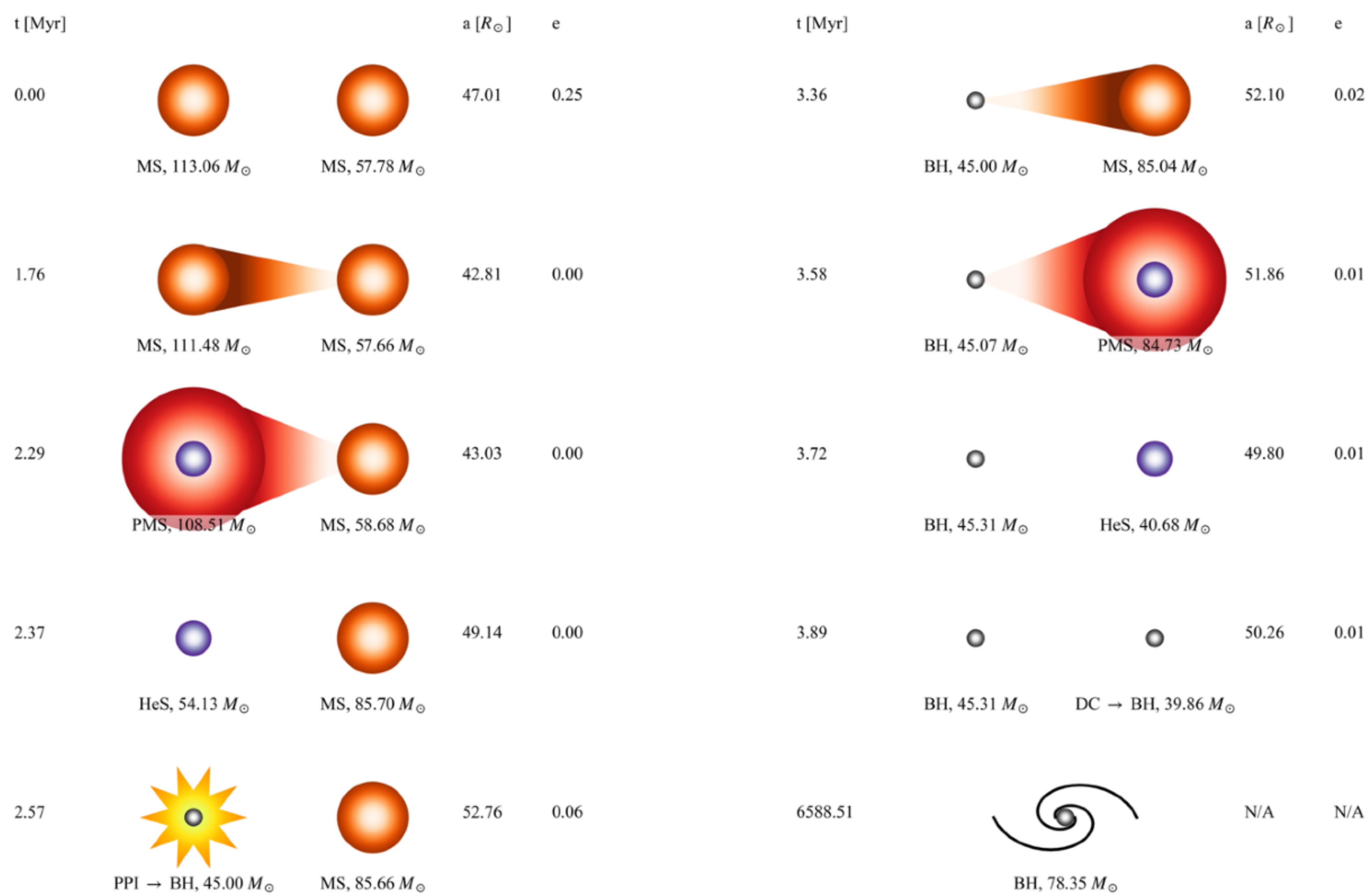

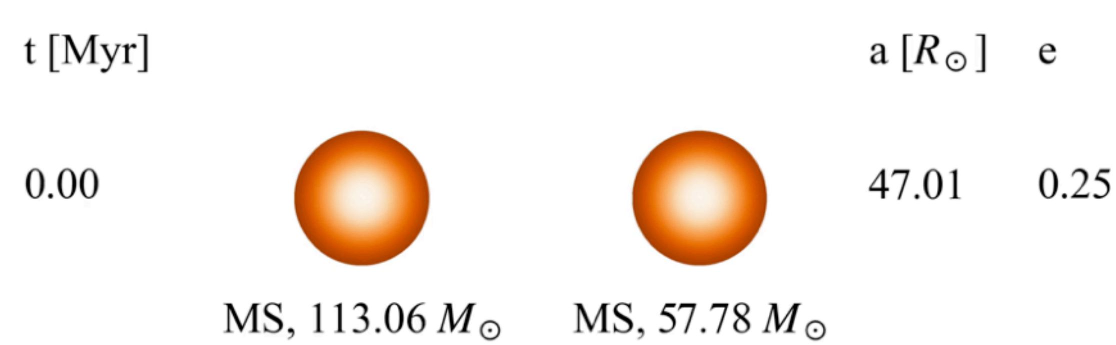

Pair instability mass gap

GWTC-1 (Abbott et al. 2019)

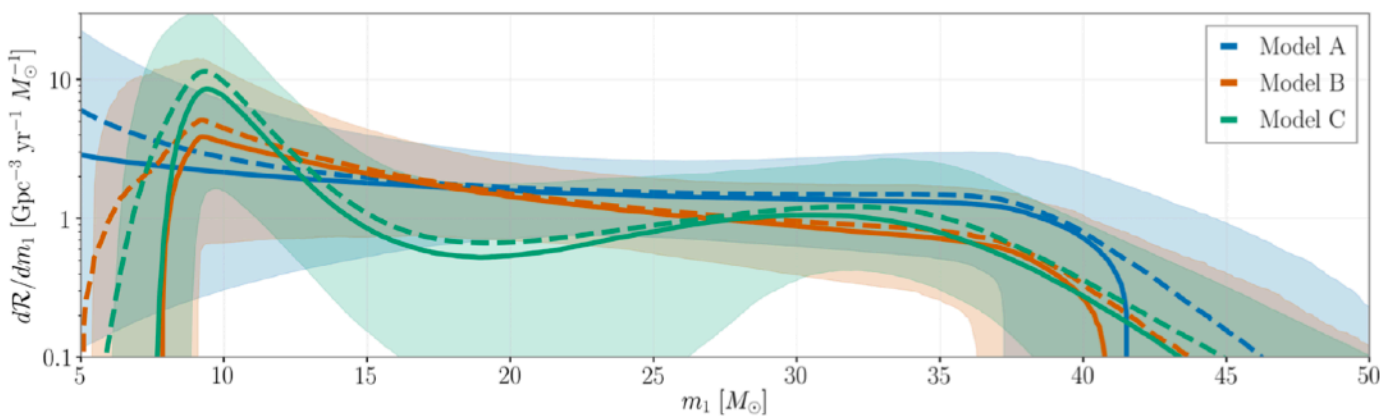

Belczynski et al. (2020)

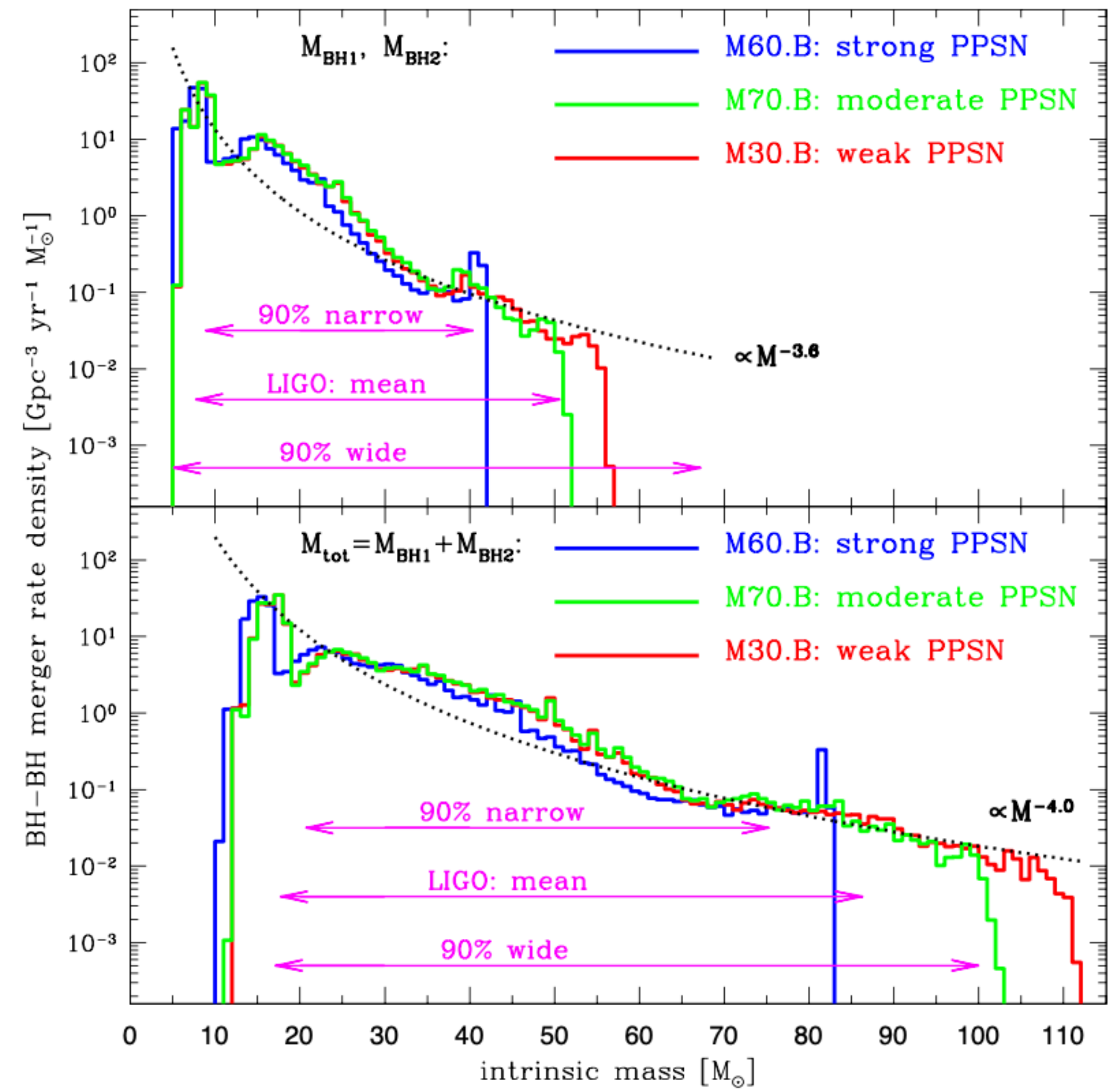

- GWTC-1 (O1/O2 results) appears to have no $\gtrsim 50M_\odot$ BH.
- This can be explained by PPISN/PISN effects and the evidence of the isolated binary scenario (Belczynski et al. 2020).

GW190521

Abbott et al. 2020

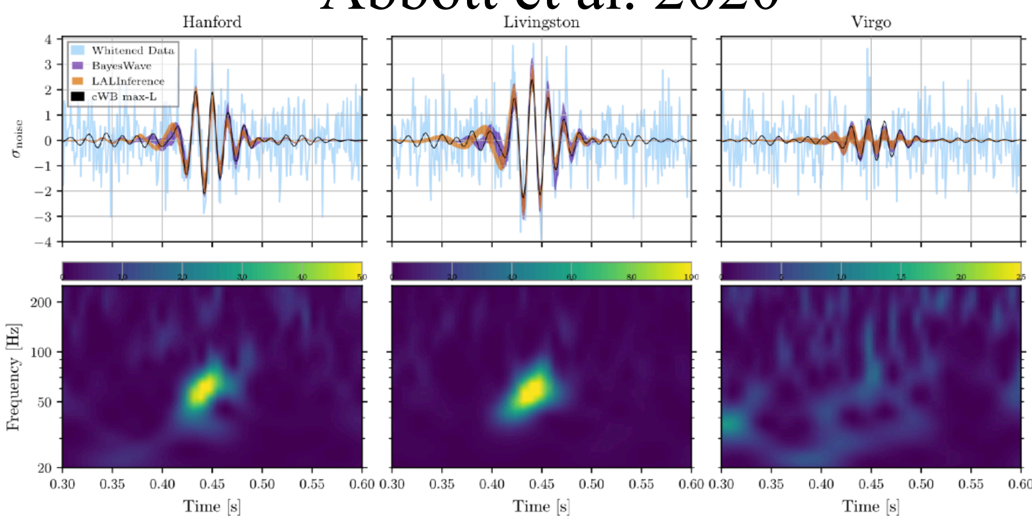

Parameter	
Primary mass	$85^{+21}_{-14}\ M_\odot$
Secondary mass	$66^{+17}_{-18}\ M_\odot$
Primary spin magnitude	$0.69^{+0.27}_{-0.62}$
Secondary spin magnitude	$0.73^{+0.24}_{-0.64}$
Total mass	$150^{+29}_{-17}\ M_\odot$
Mass ratio ($m_2/m_1 \le 1$)	$0.79^{+0.19}_{-0.29}$
Effective inspiral spin parameter (χ_{eff})	$0.08^{+0.27}_{-0.36}$
Effective precession spin parameter (χ_{p})	$0.68^{+0.25}_{-0.37}$
Luminosity Distance	$5.3^{+2.4}_{-2.6}$ Gpc
Redshift	$0.82^{+0.28}_{-0.34}$
Final mass	$142^{+28}_{-16}\ M_\odot$
Final spin	$0.72^{+0.09}_{-0.12}$
$P\ (m_1 < 65\ M_\odot)$	0.32%
$\log_{10}$ Bayes factor for orbital precession	$1.06^{+0.06}_{-0.06}$
$\log_{10}$ Bayes factor for nonzero spins	$0.92^{+0.06}_{-0.06}$
$\log_{10}$ Bayes factor for higher harmonics	$-0.38^{+0.06}_{-0.06}$

GWTC-1 (Abbott et al. 2019)

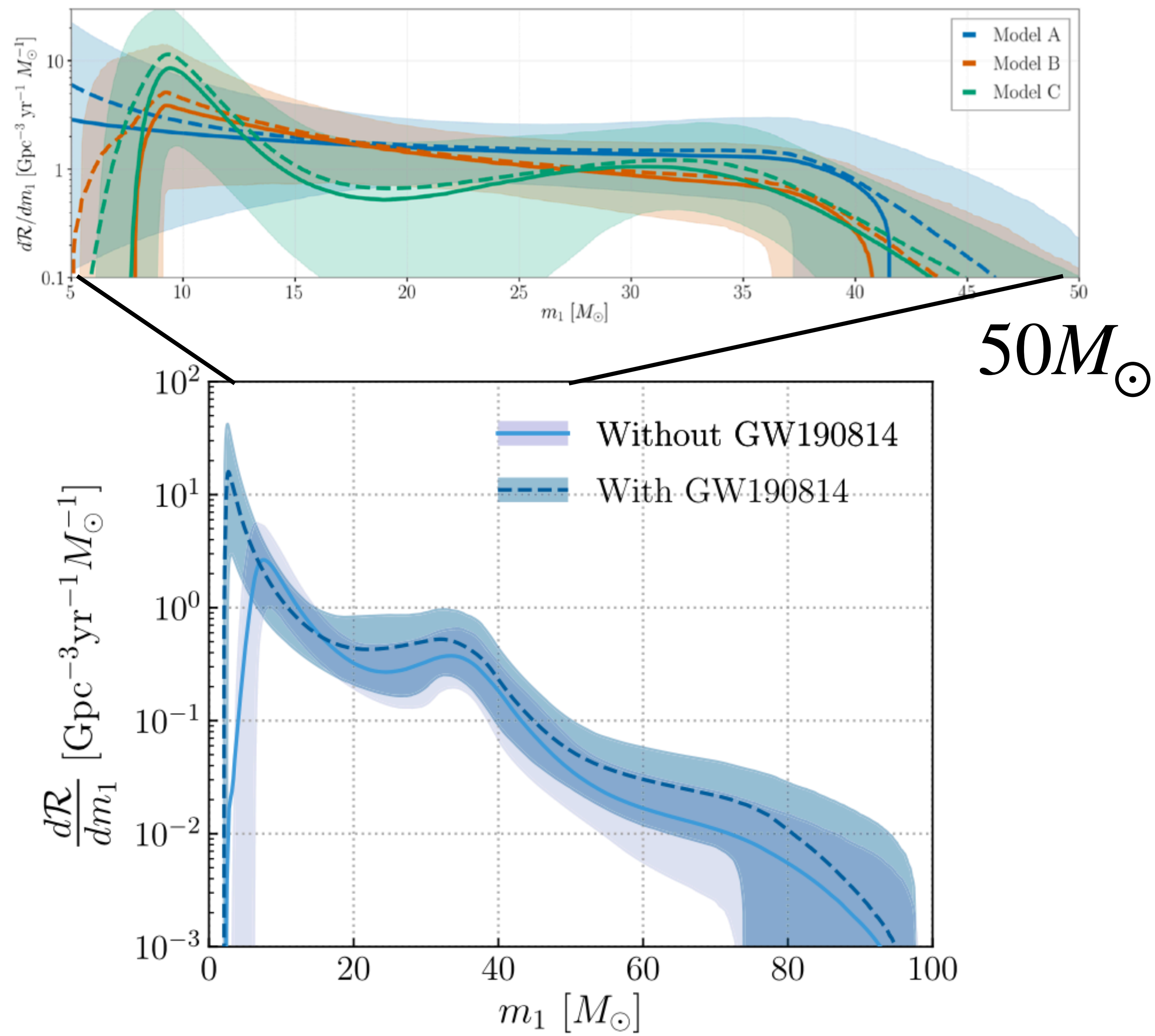

GWTC-2 (Abbott et al. 2021)

Cluster origin?

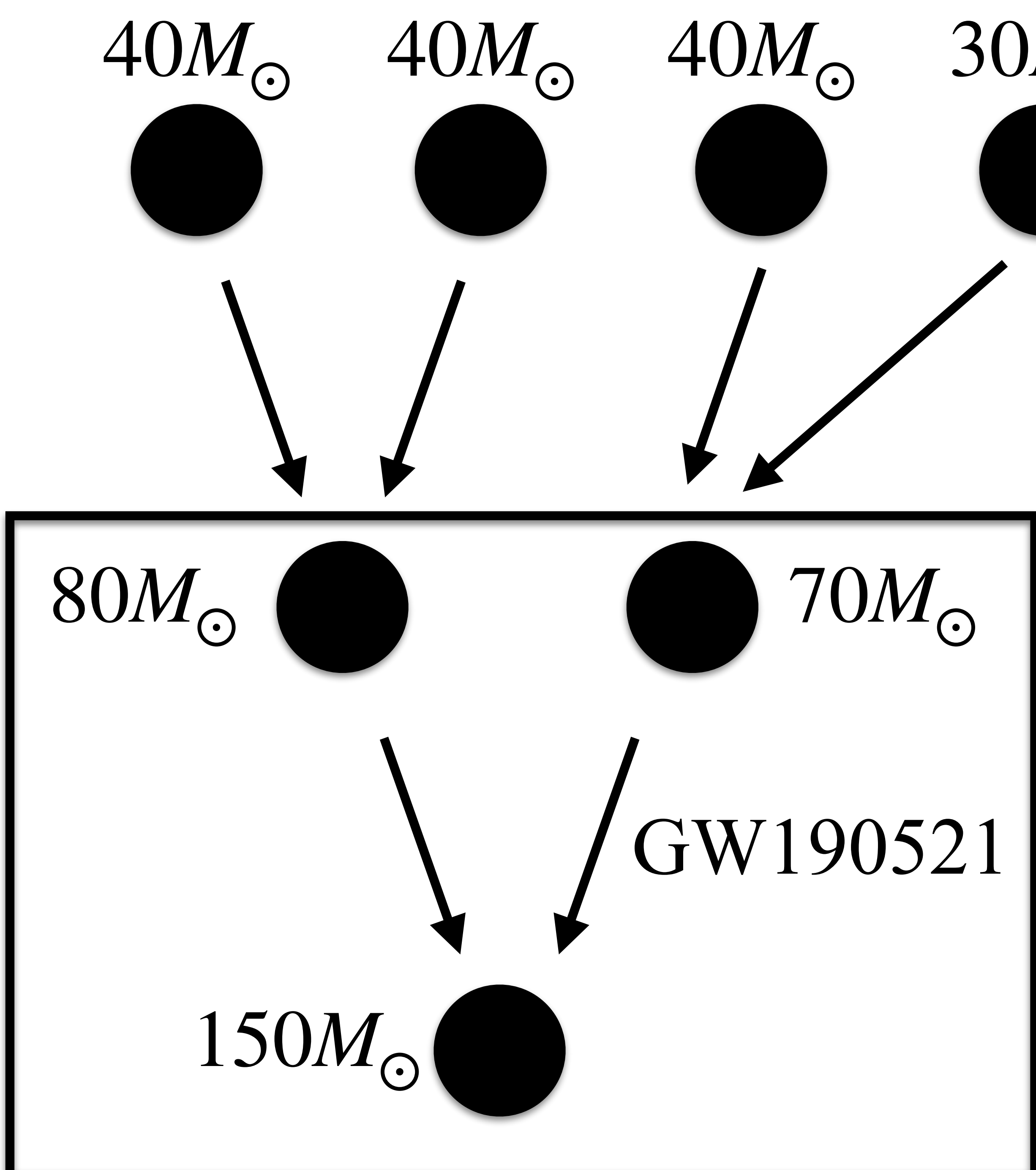

Globular clusters (Rodriguez et al. 2019)

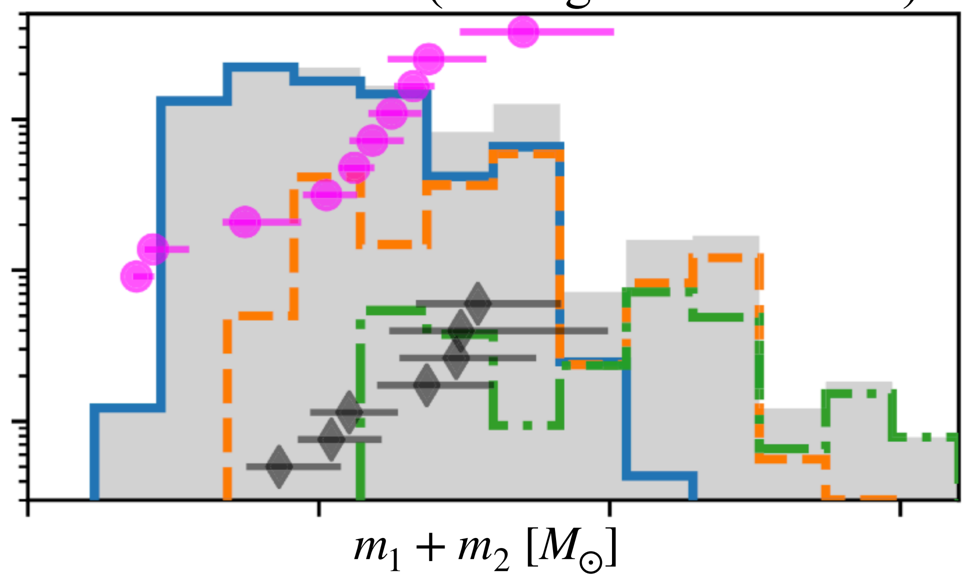

Open clusters (Santoliquido et al. 2020)

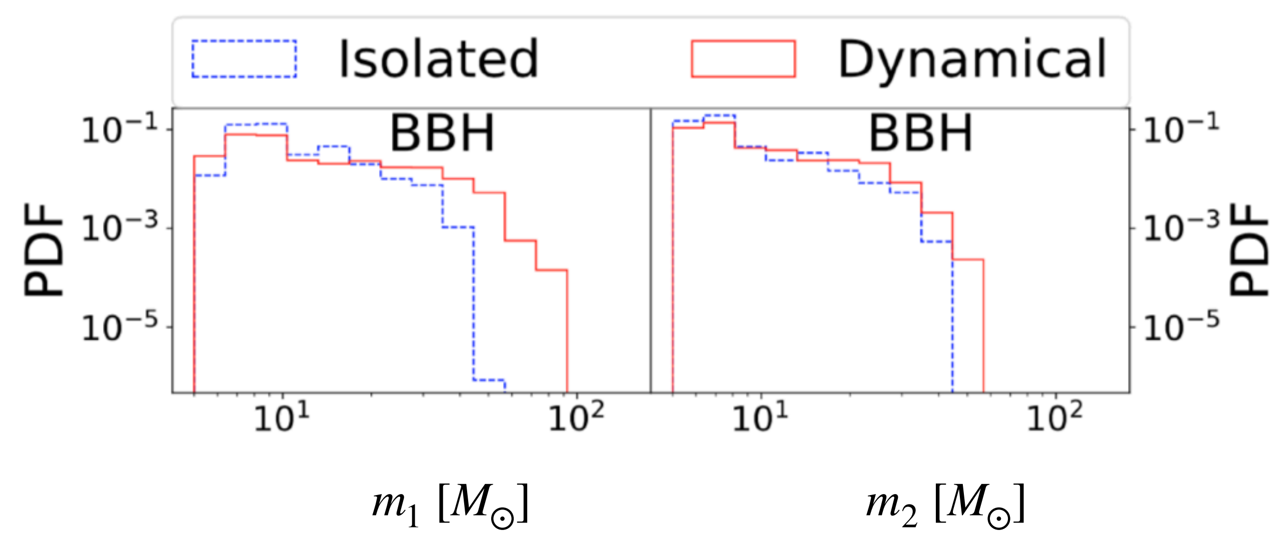

See also AGN disks (Tagawa et al. 2020)

$^{12}C(\alpha,\gamma)^{16}O$ reaction rate

Farmer et al. (2020)

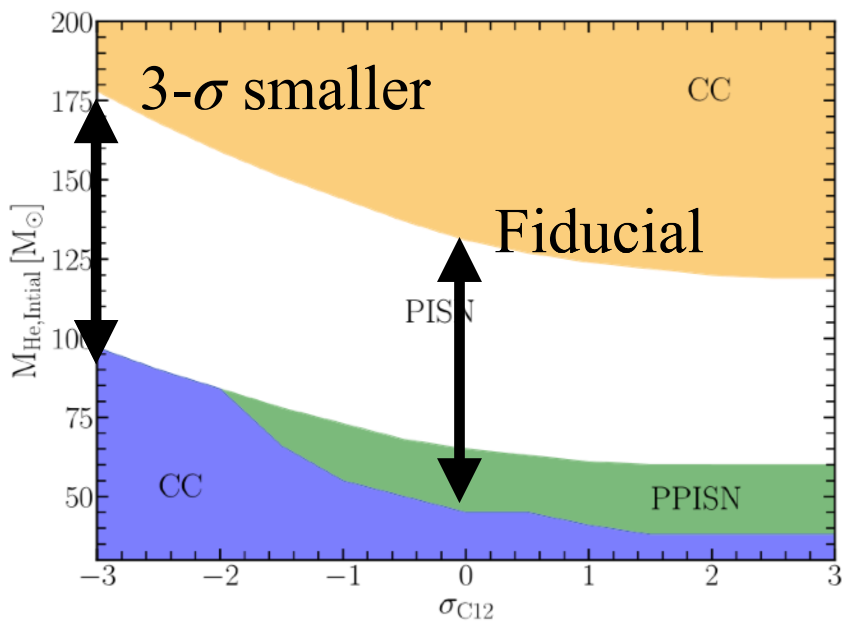

Takahashi (2018)

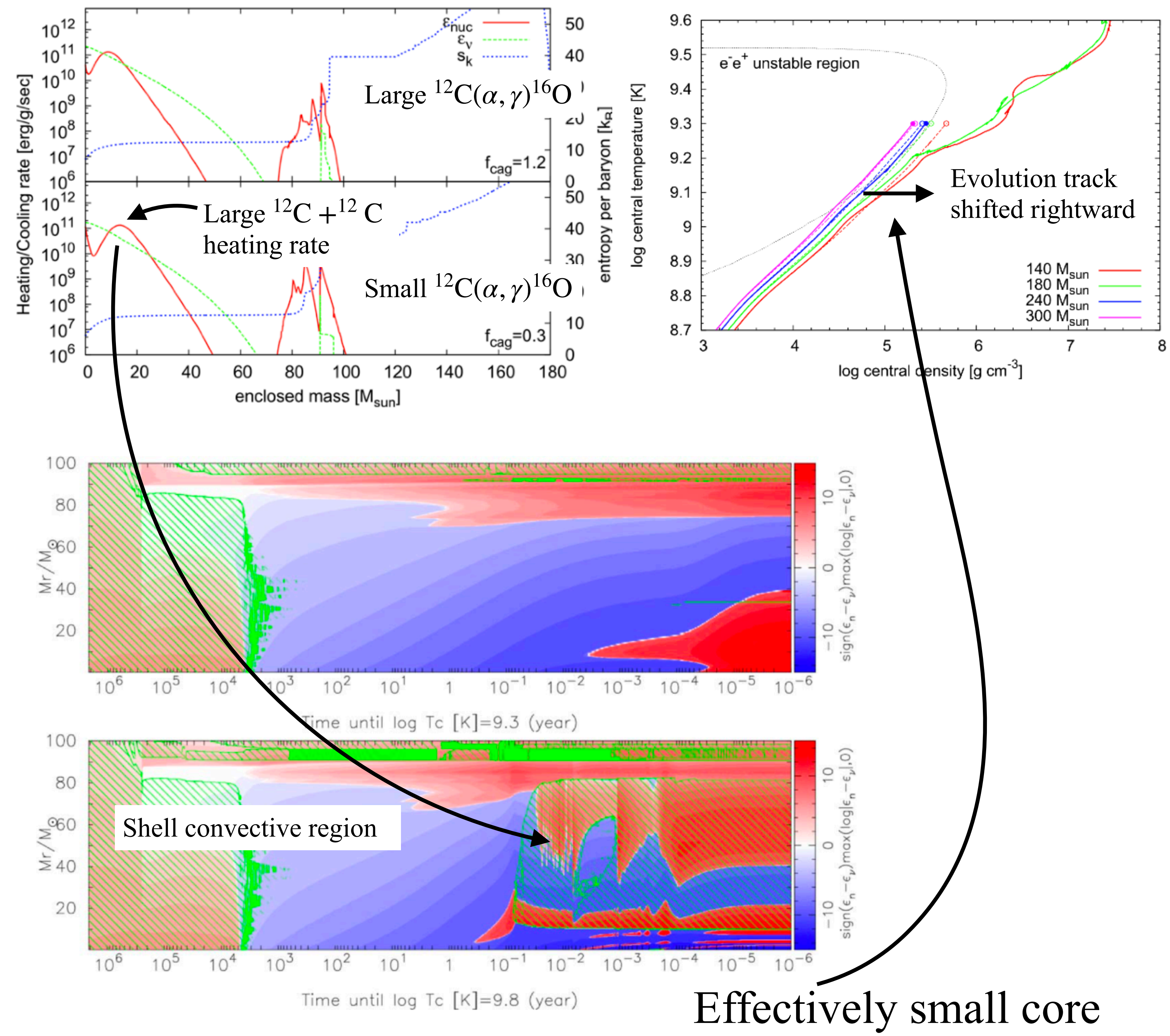

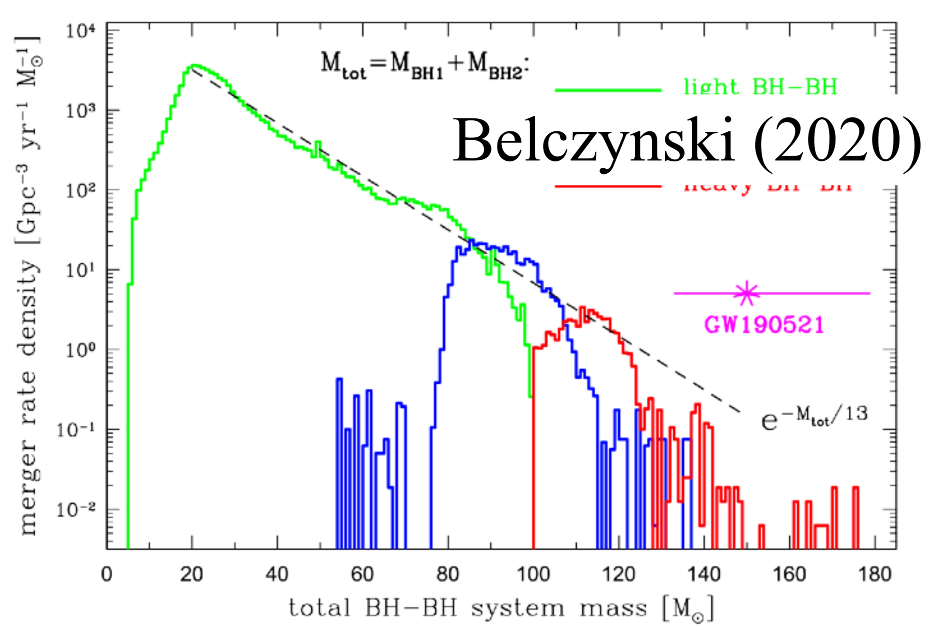

Extremely metal poor stars

$0Z_{\odot}$

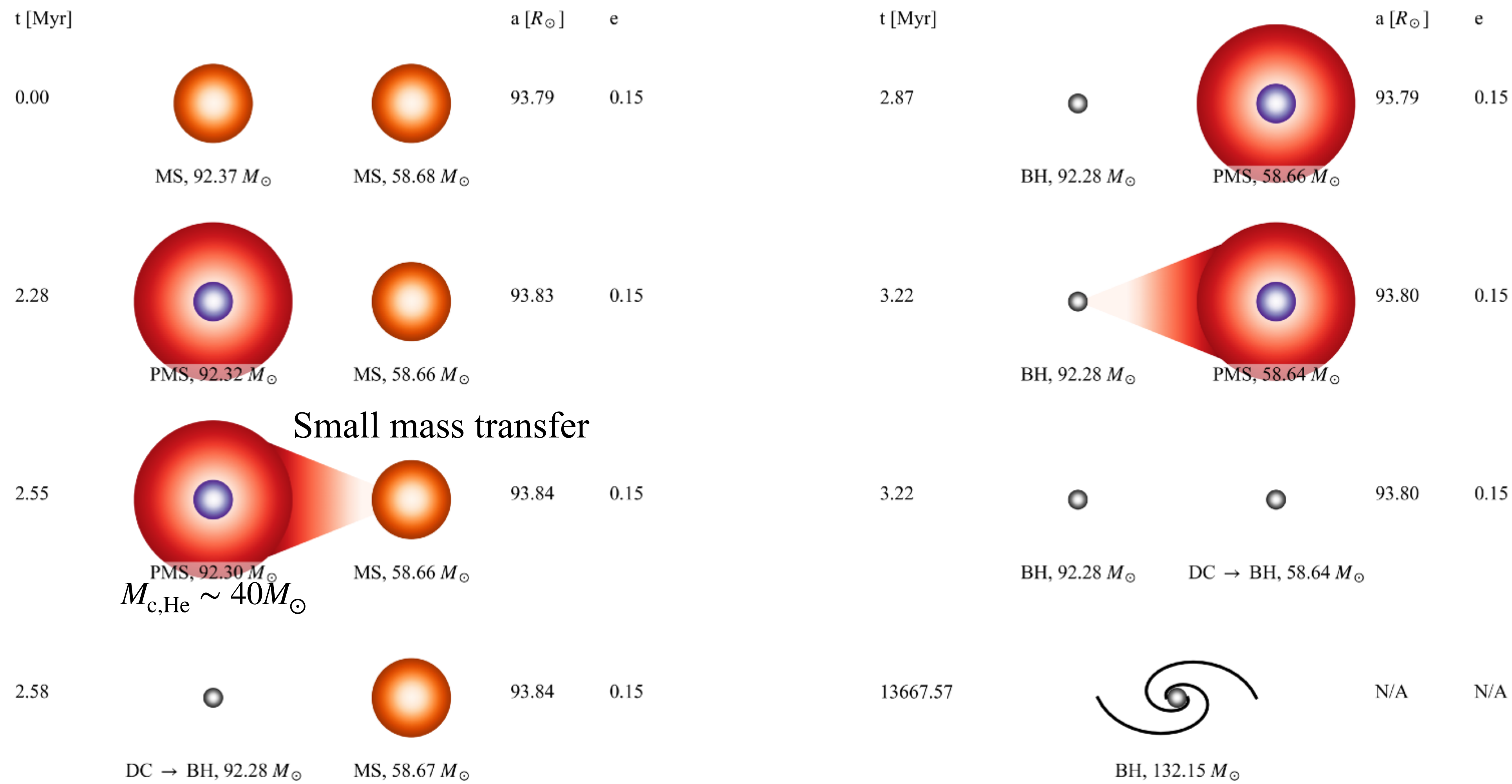

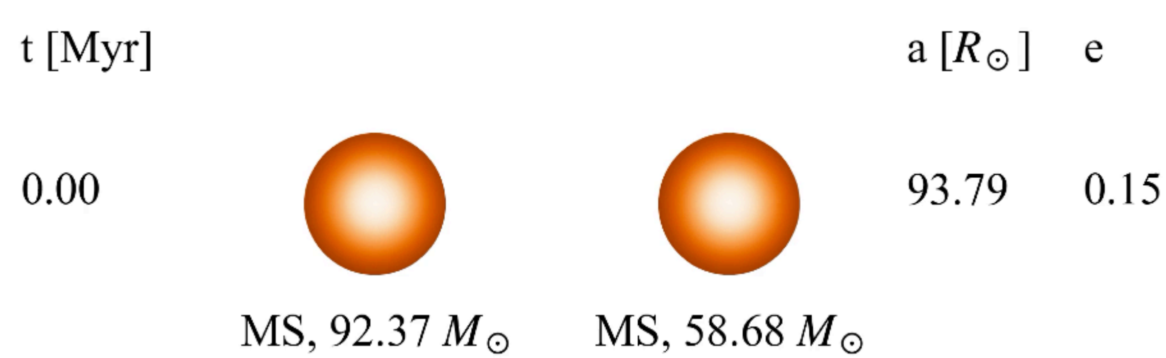

Tanikawa et al. (2021, MNRAS, 495, 4170)

Our previous study

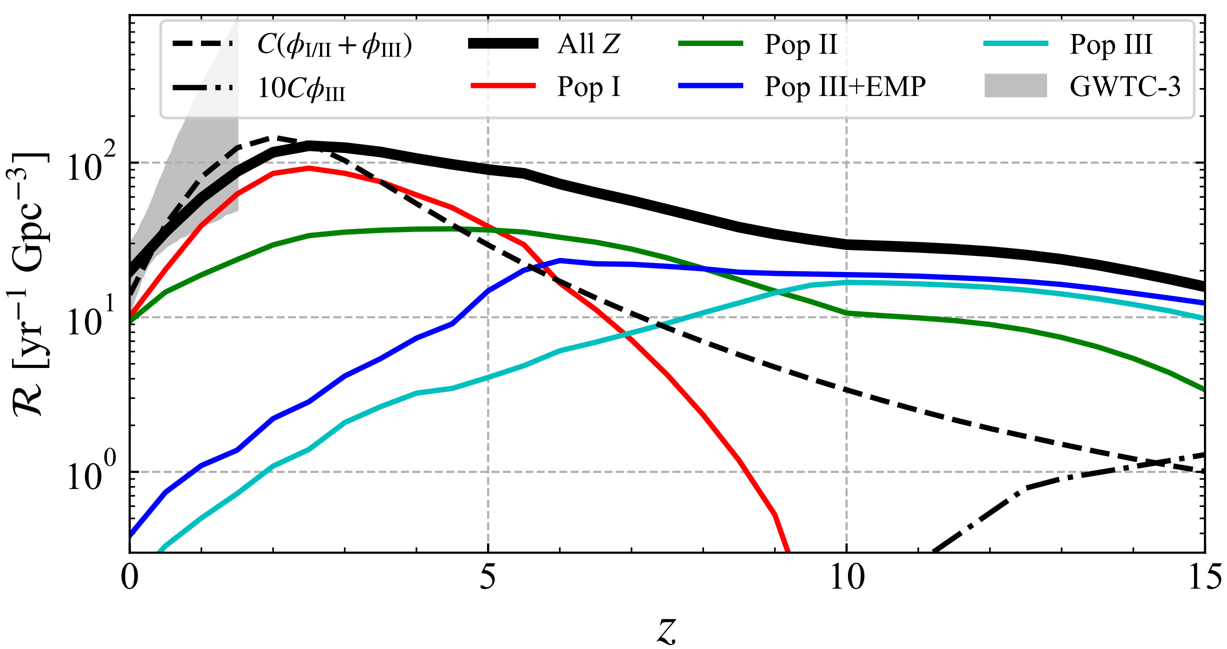

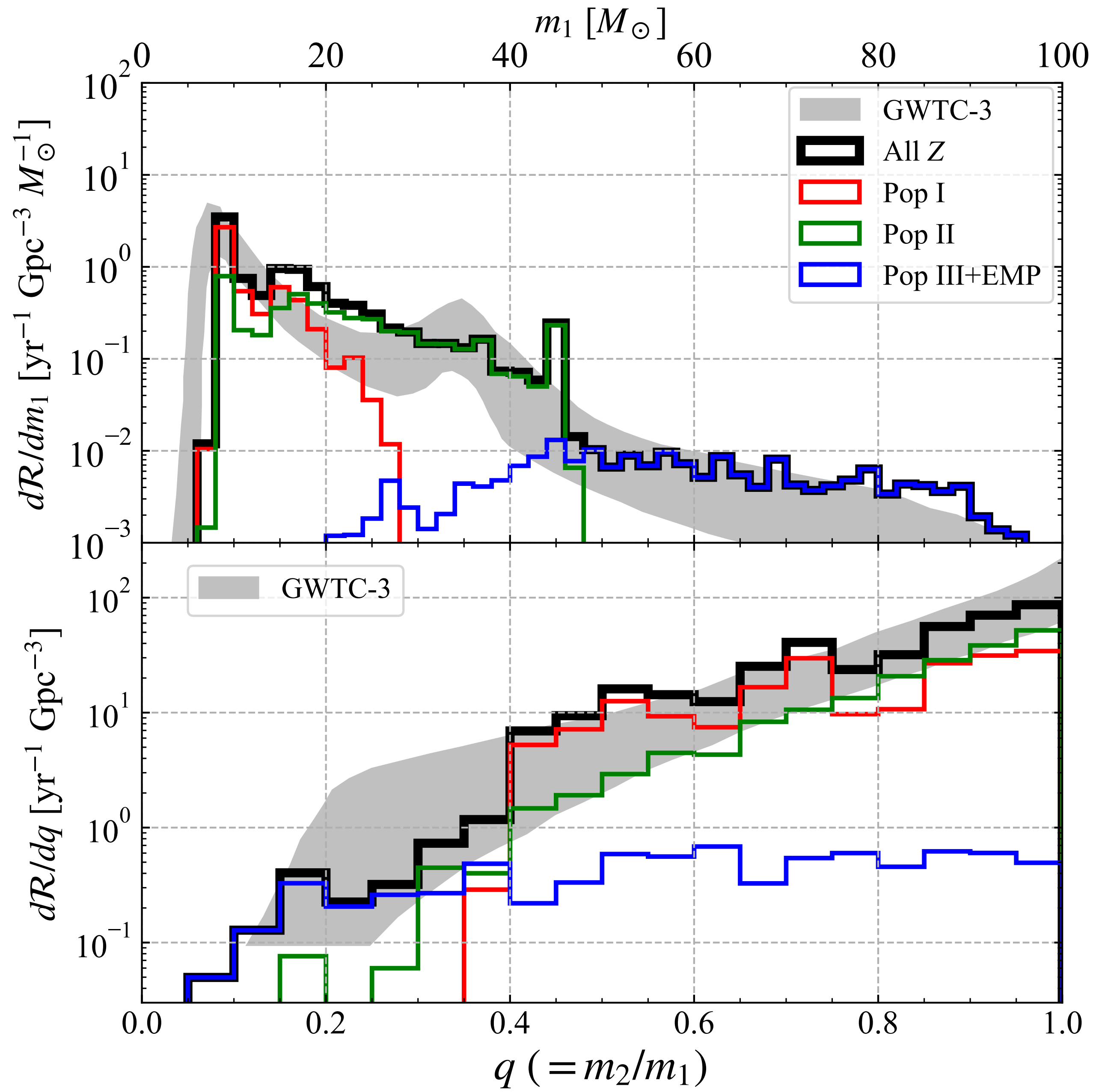

Tanikawa et al. (2022, ApJ, 910, 30)

Short summary

- The isolated binary scenario still survives.
- We realized that the $^{12}\mathrm{C}(\alpha,\gamma)^{16}\mathrm{O}$ reaction rate is one of the most important parameters for shaping the BH mass distribution via PISNe, despite that the fiducial and 3-σ smaller ones can explain GWTC-3 results.
- The PISN event rate should be strongly dependent on the $^{12}\mathrm{C}(\alpha,\gamma)^{16}\mathrm{O}$ reaction rate.
- We investigated if the PISN detection number depends on the $^{12}\mathrm{C}(\alpha,\gamma)^{16}\mathrm{O}$ reaction rate by binary population synthesis simulation.

Binary population synthesis

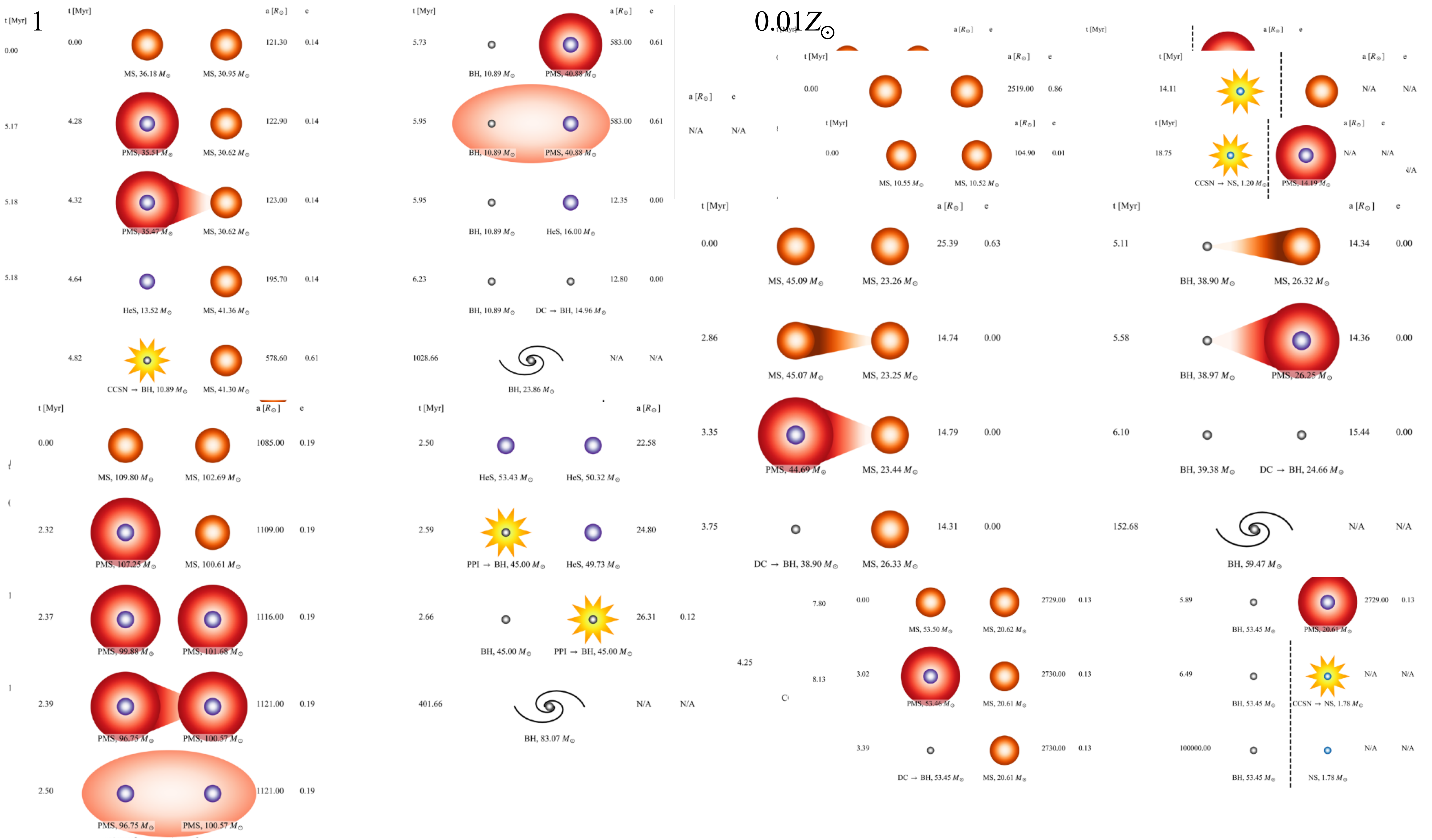

Initial conditions

Star formation history

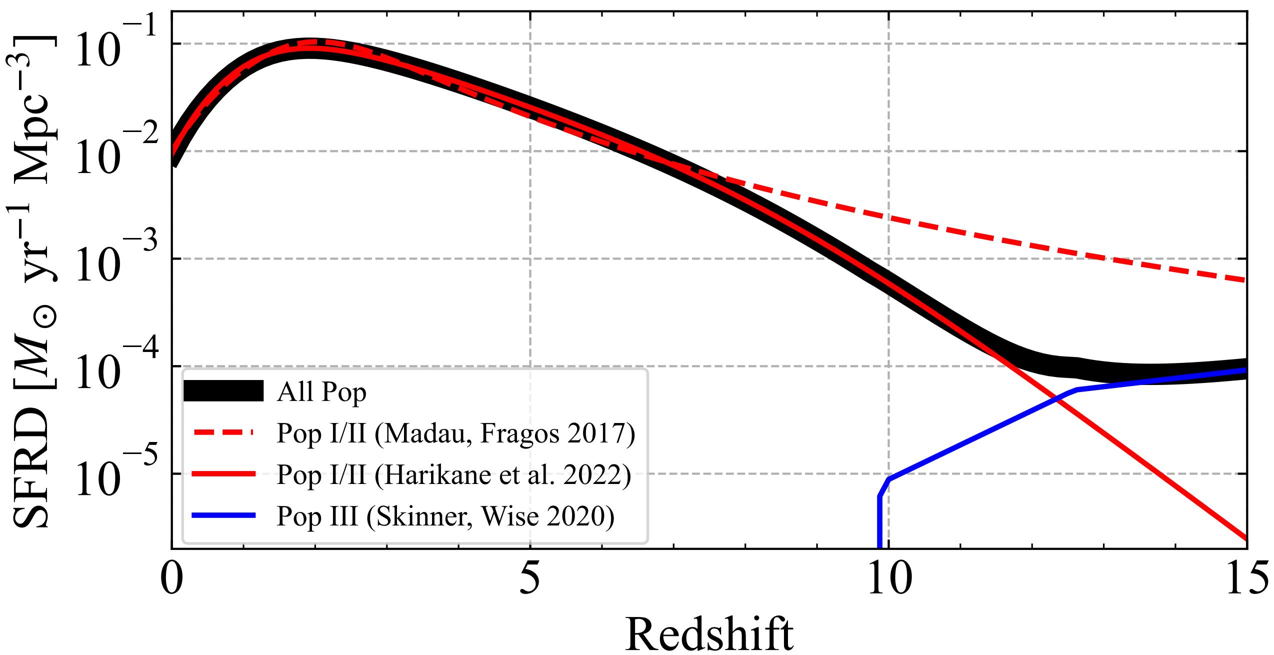

Metallicity evolution (Pop I/II)

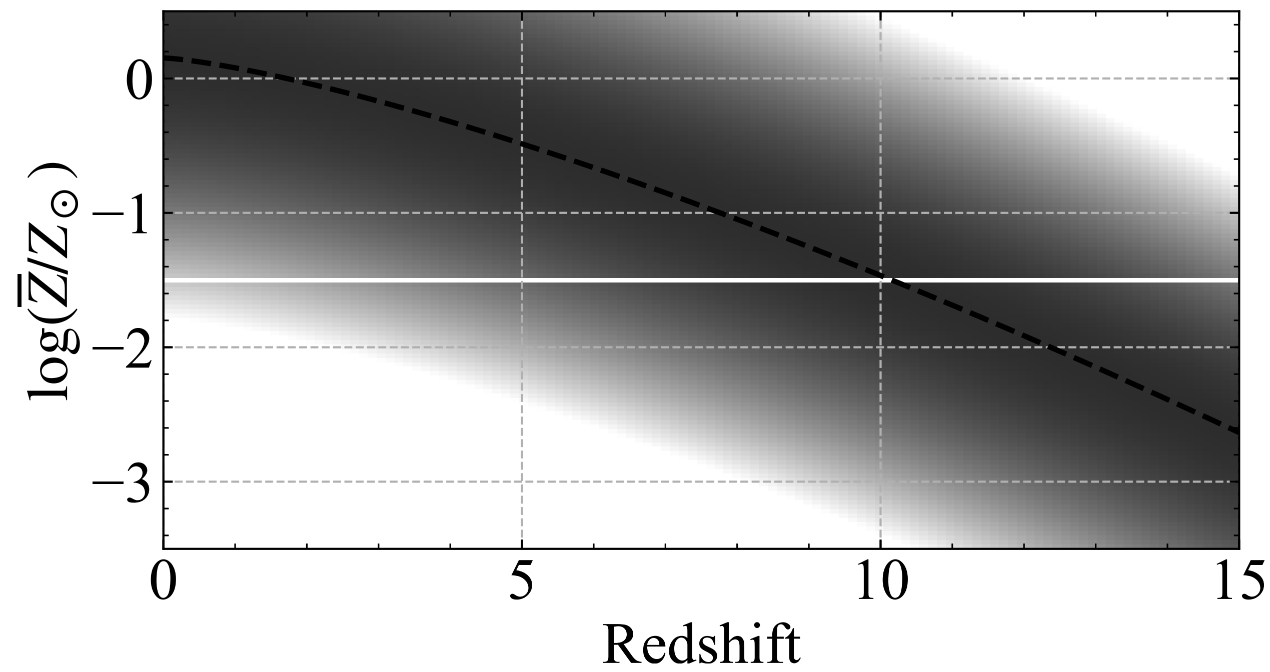

Initial stellar mass function (IMF)

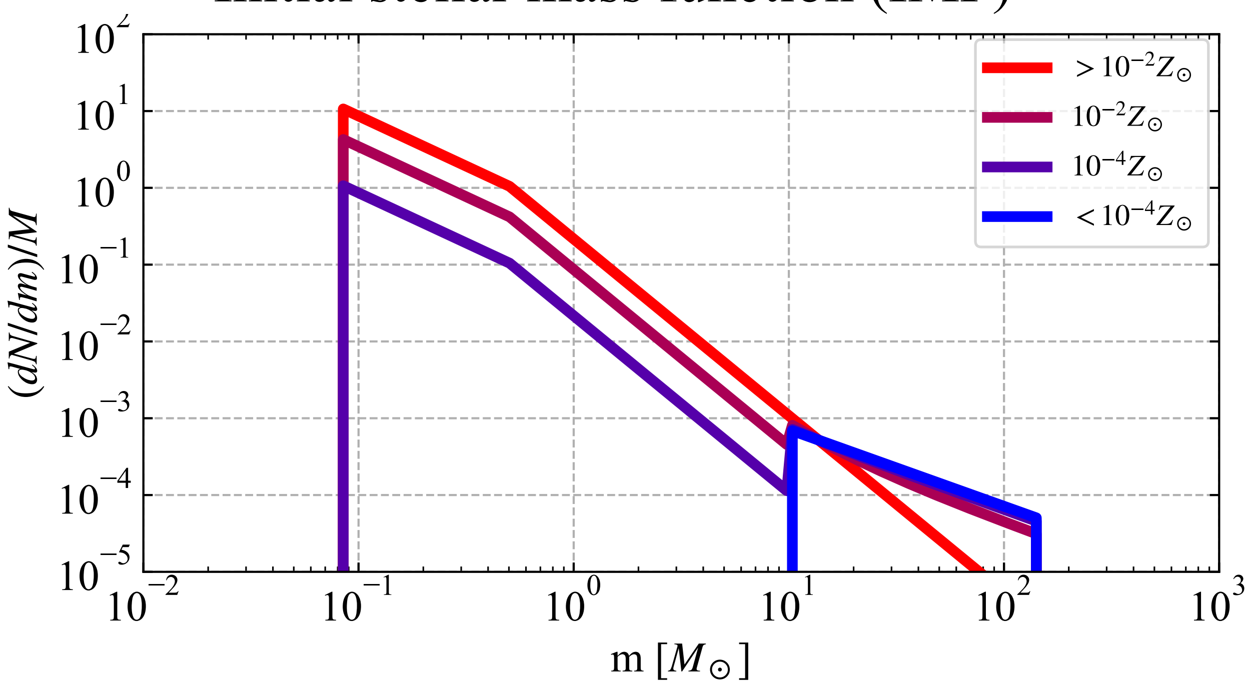

Binary initial conditions

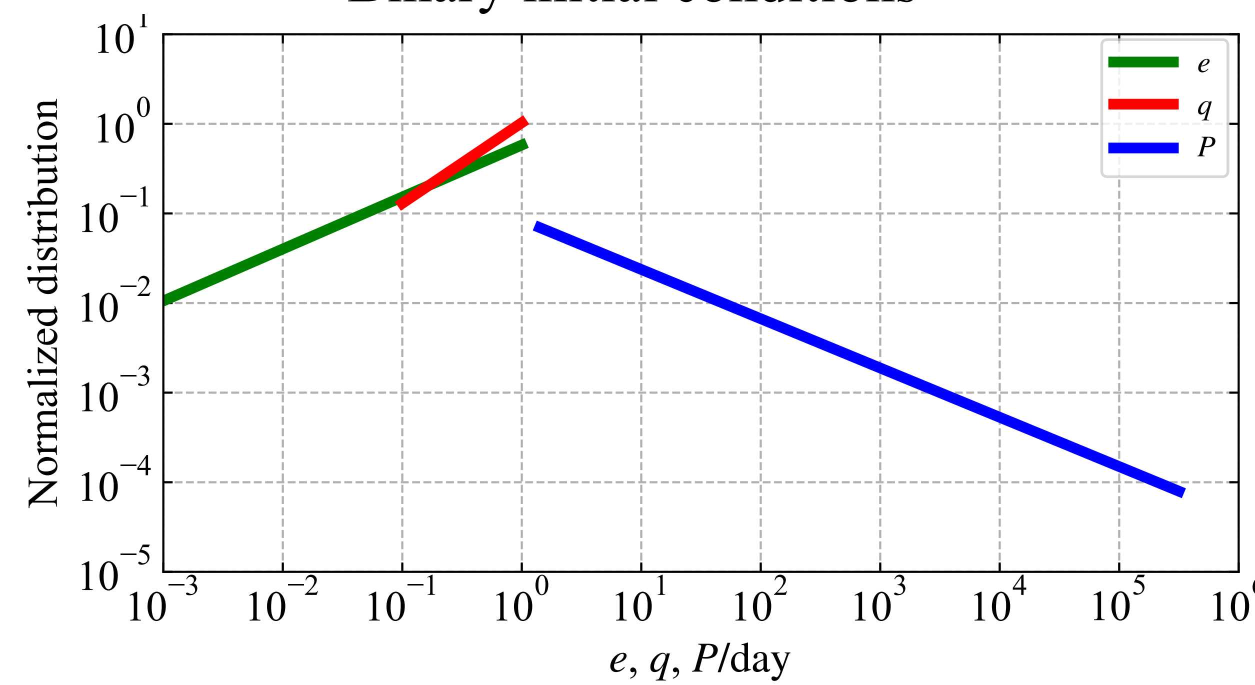

Single star evolution model

- Evolution track
  - Hurley's model for $> 0.1Z_{\odot}$
  - Tanikawa's model for $\leq 0.1Z_{\odot}$
- Belczynski's stellar winds
- Fryer's rapid supernova model with Leung's PISN/PPISN model
- Fallback BH natal kick (265km/s for NS)

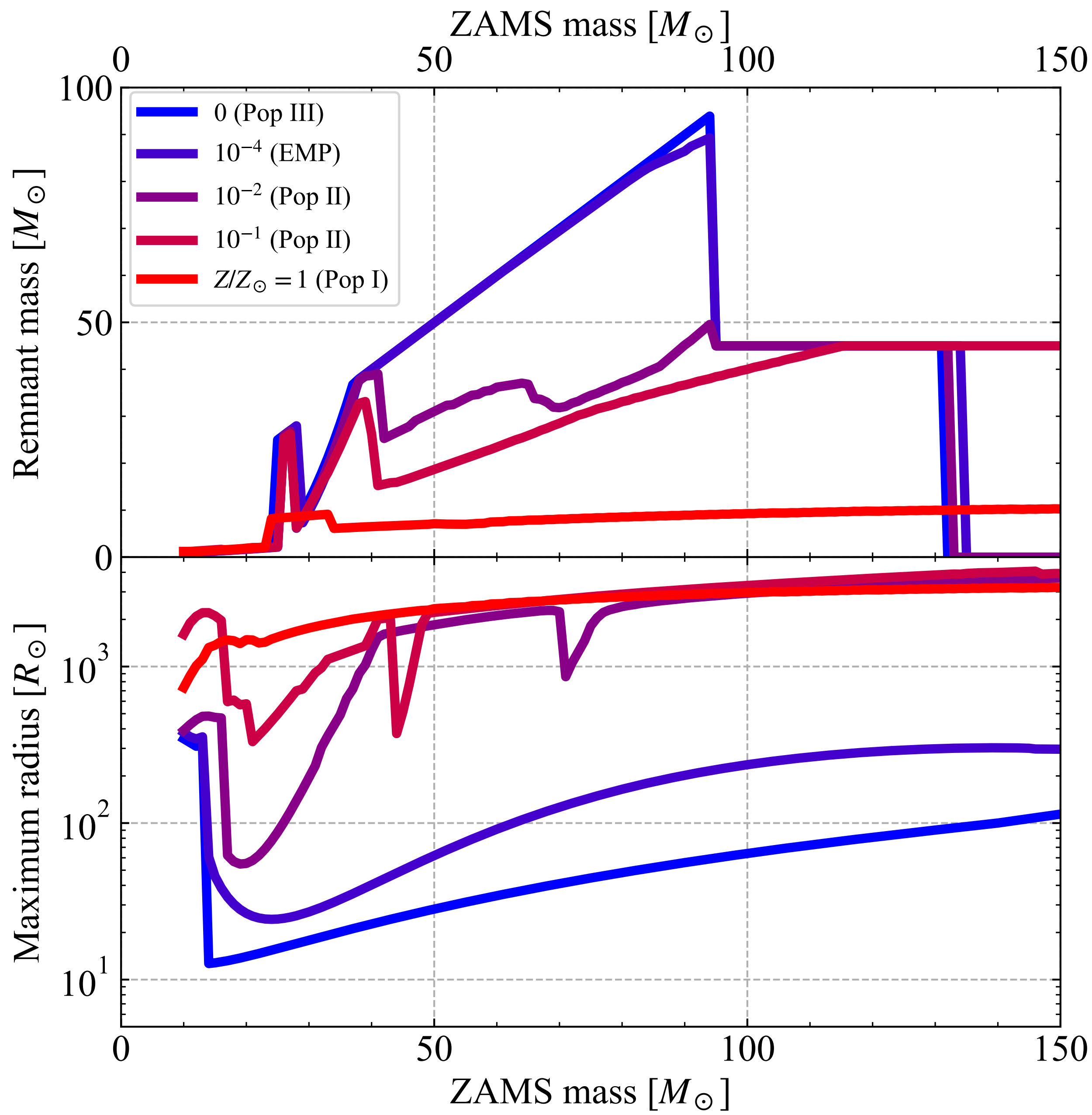

Binary star evolution model

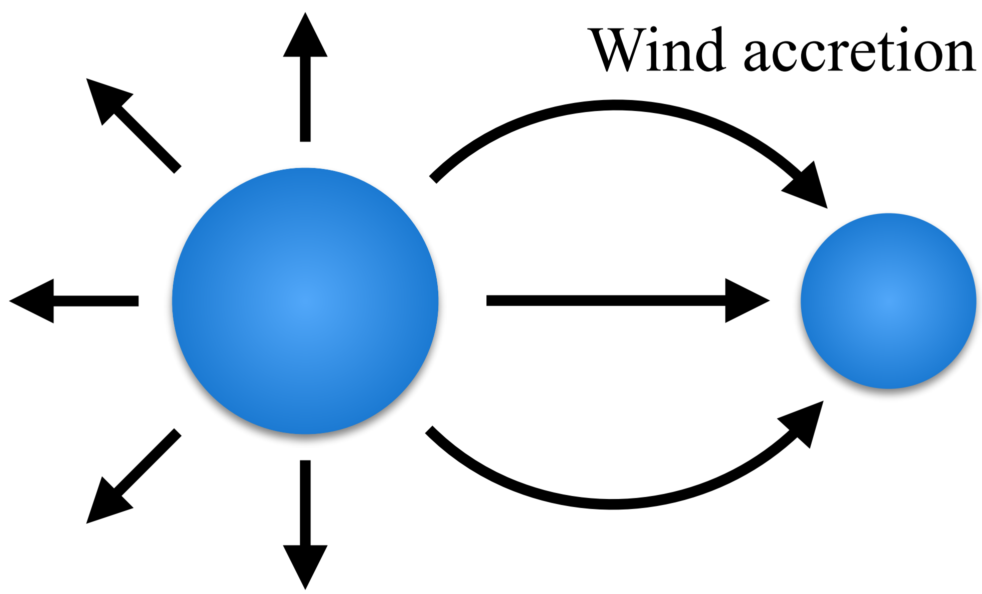

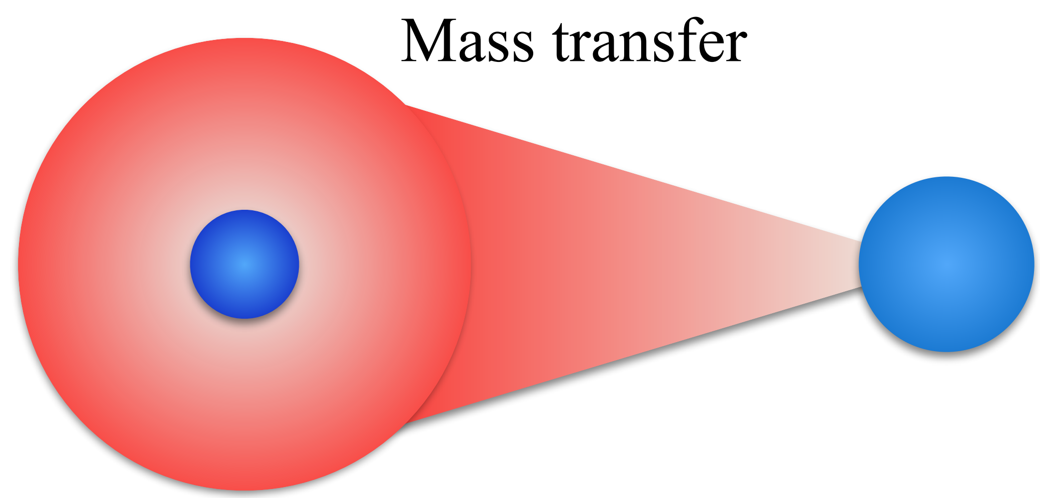

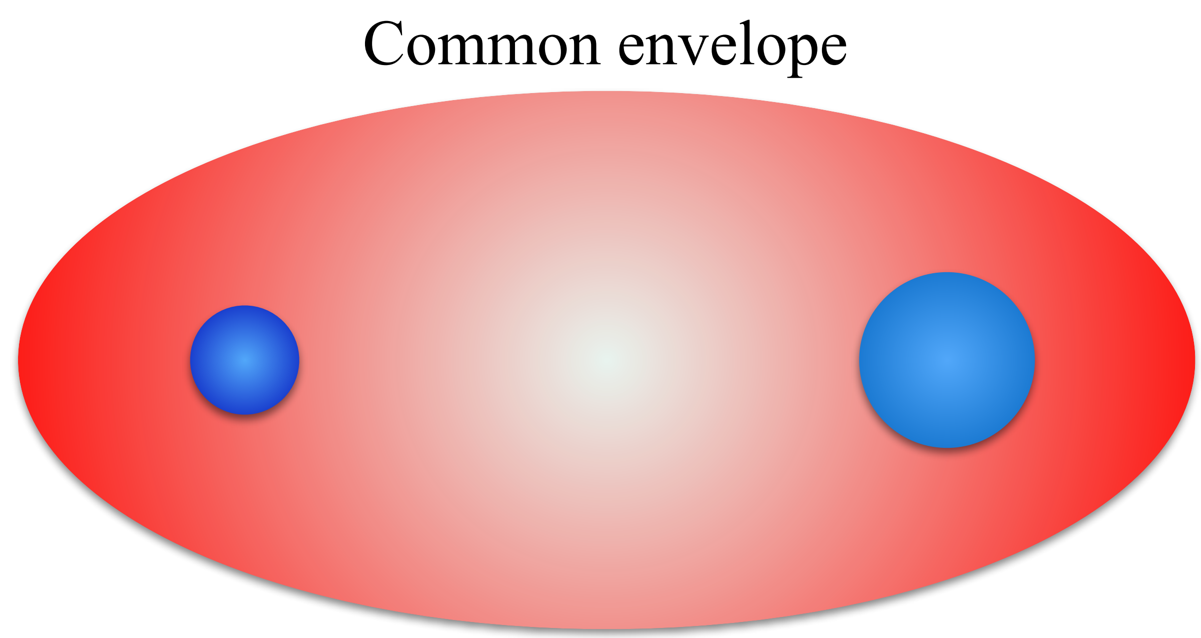

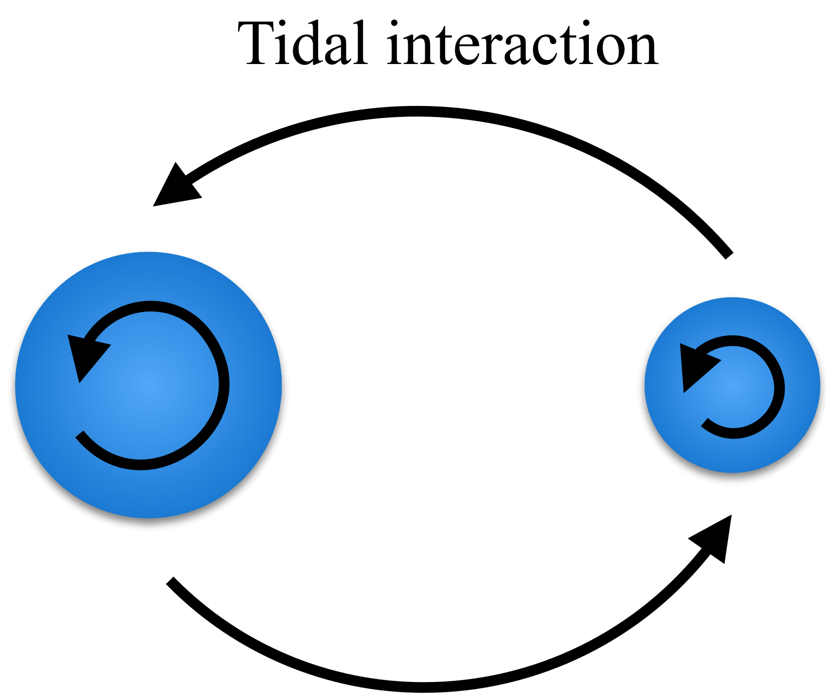

- Magnetic braking
- Orbital decay due to gravitational wave
- etc.

Variety of parameters

- Different PISN models
  - Fiducial
    - PPISN: $M_{\mathrm{c,He}} = 45 - 65 M_\odot$
    - PISN: $M_{\mathrm{c,He}} = 65 - 135 M_\odot$
  - 3-σ
    - PPISN: N/A
    - PISN: $M_{\mathrm{c,He}} = 90 - 180 M_\odot$
- Different maximum masses
  - 150, 300, 600 $M_\odot$

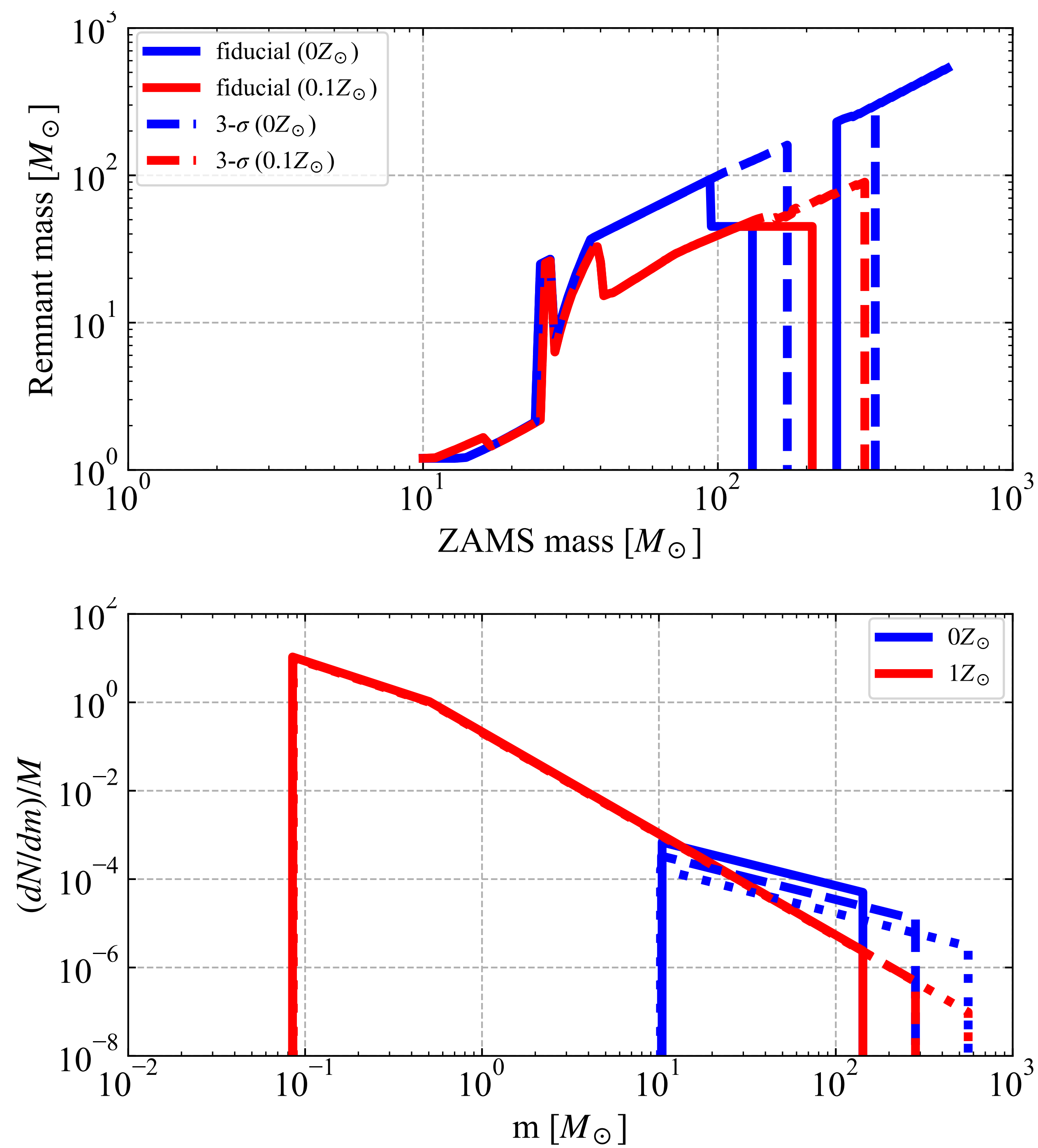

Consistency check

- BH-BH Merger rate
- Primary BH mass distribution

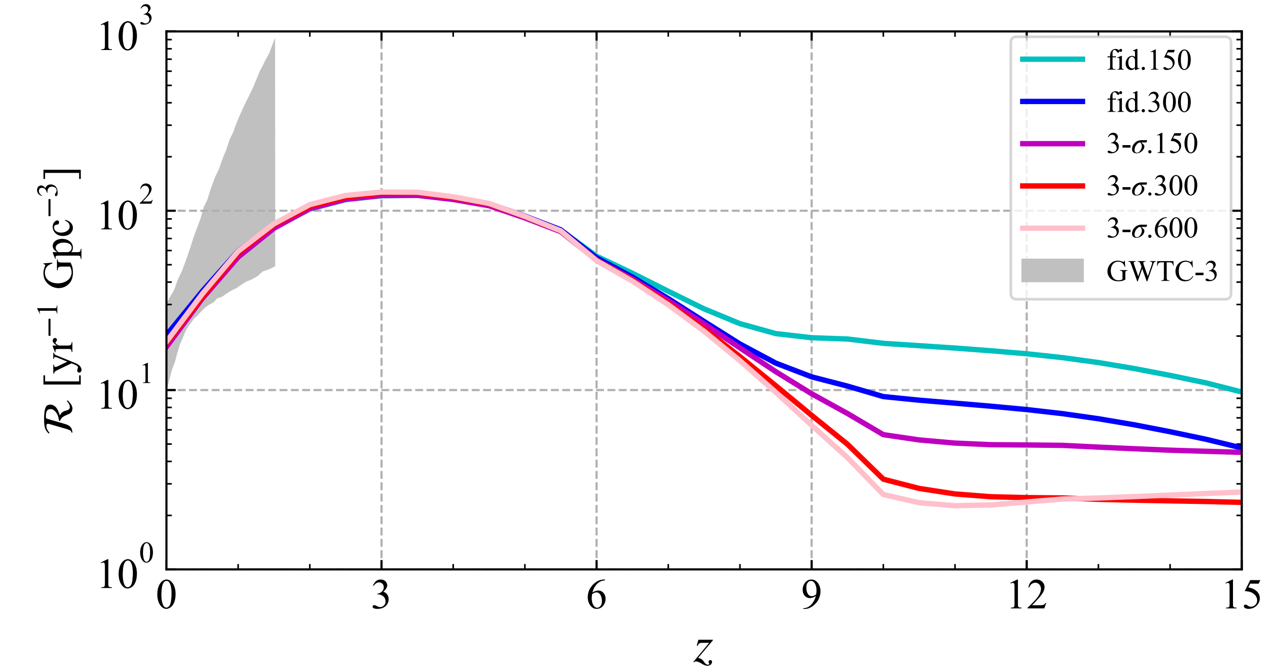

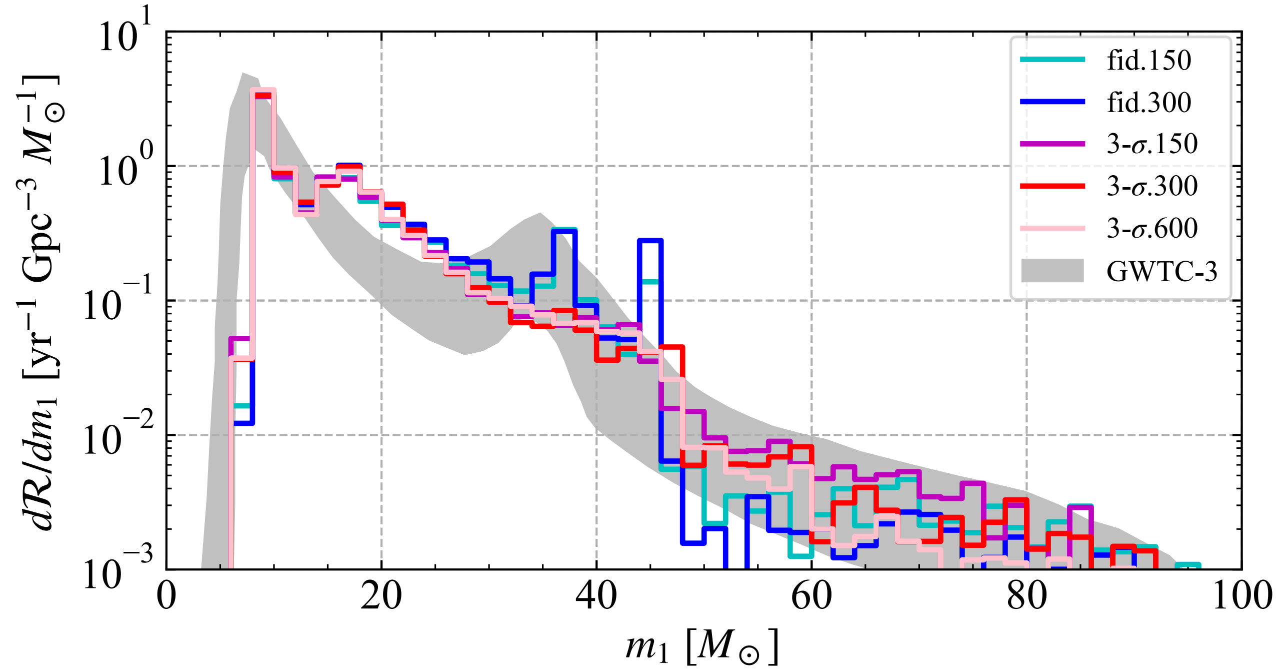

PISN event rate

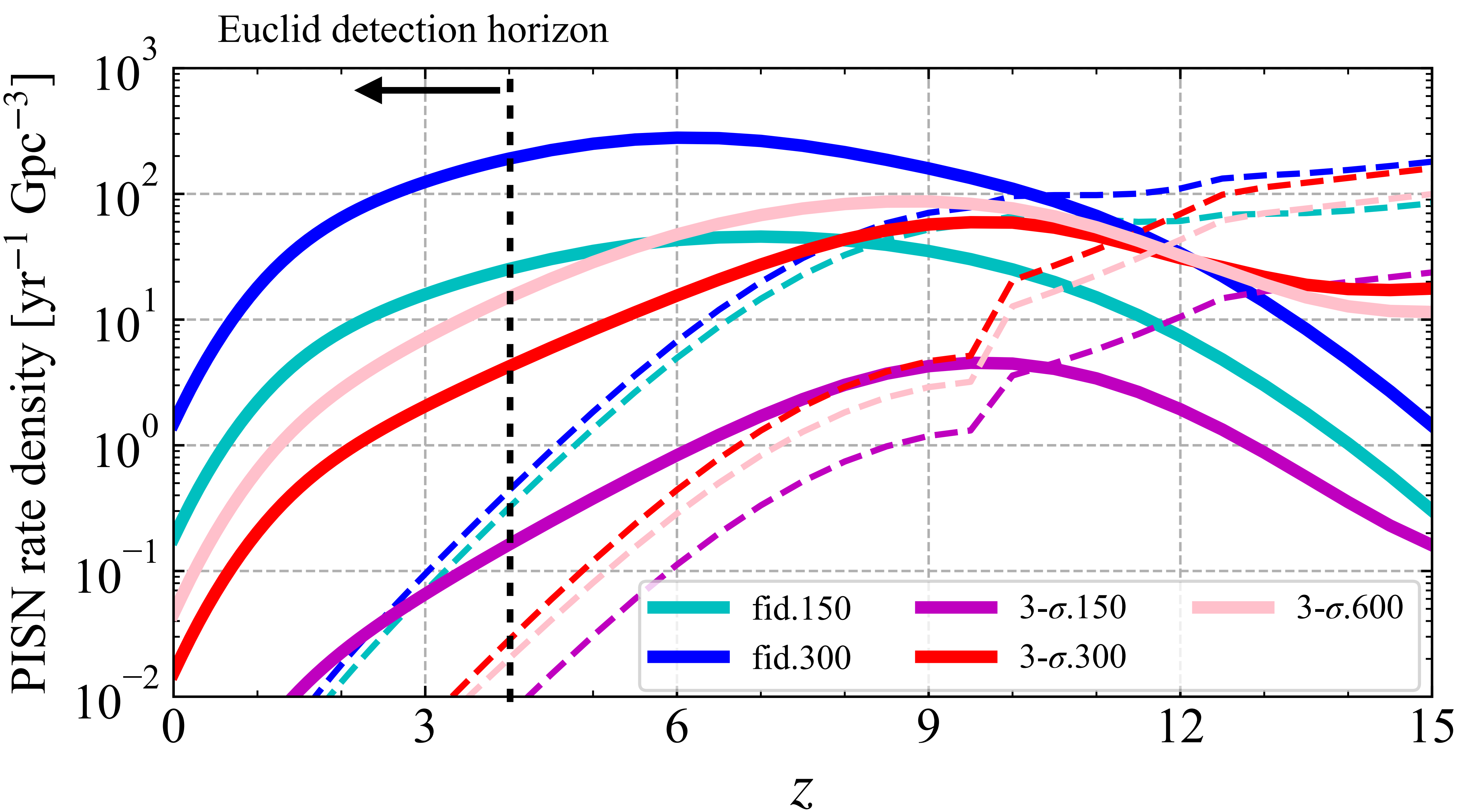

Solid: type I (hydrogen-poor) PISN, dashed: type II (hydrogen-rich) PISN)

Euclid space telescope

- To be launched 2023 by ESA
  - Postponed because of Soyuz → Ariane
- The Sun-Earth L2 (the same as JWST)
- 1.2-m telescope

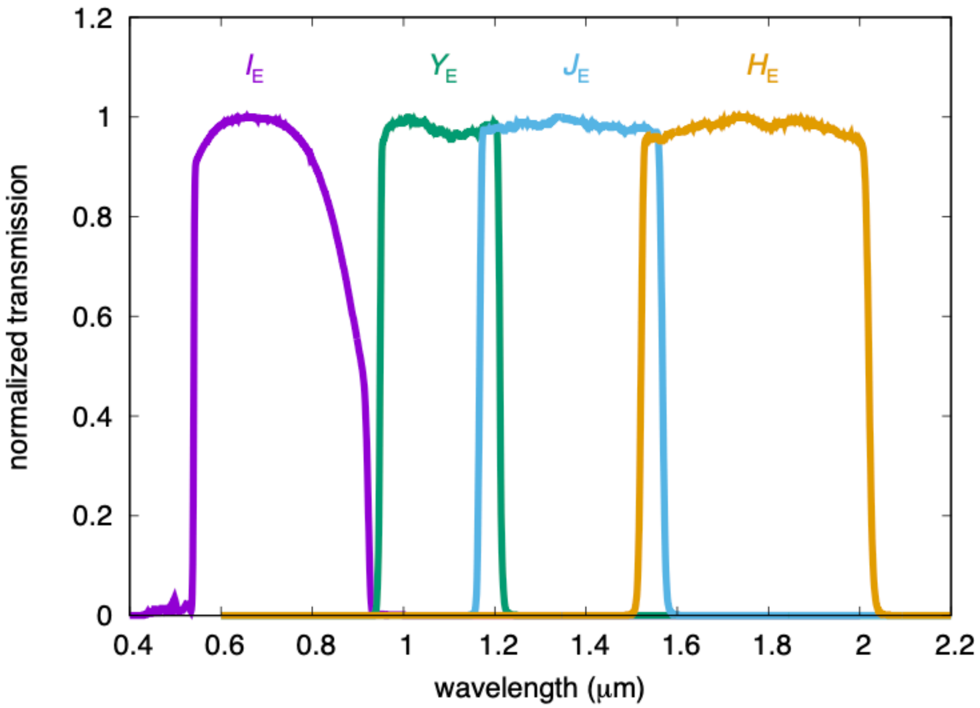

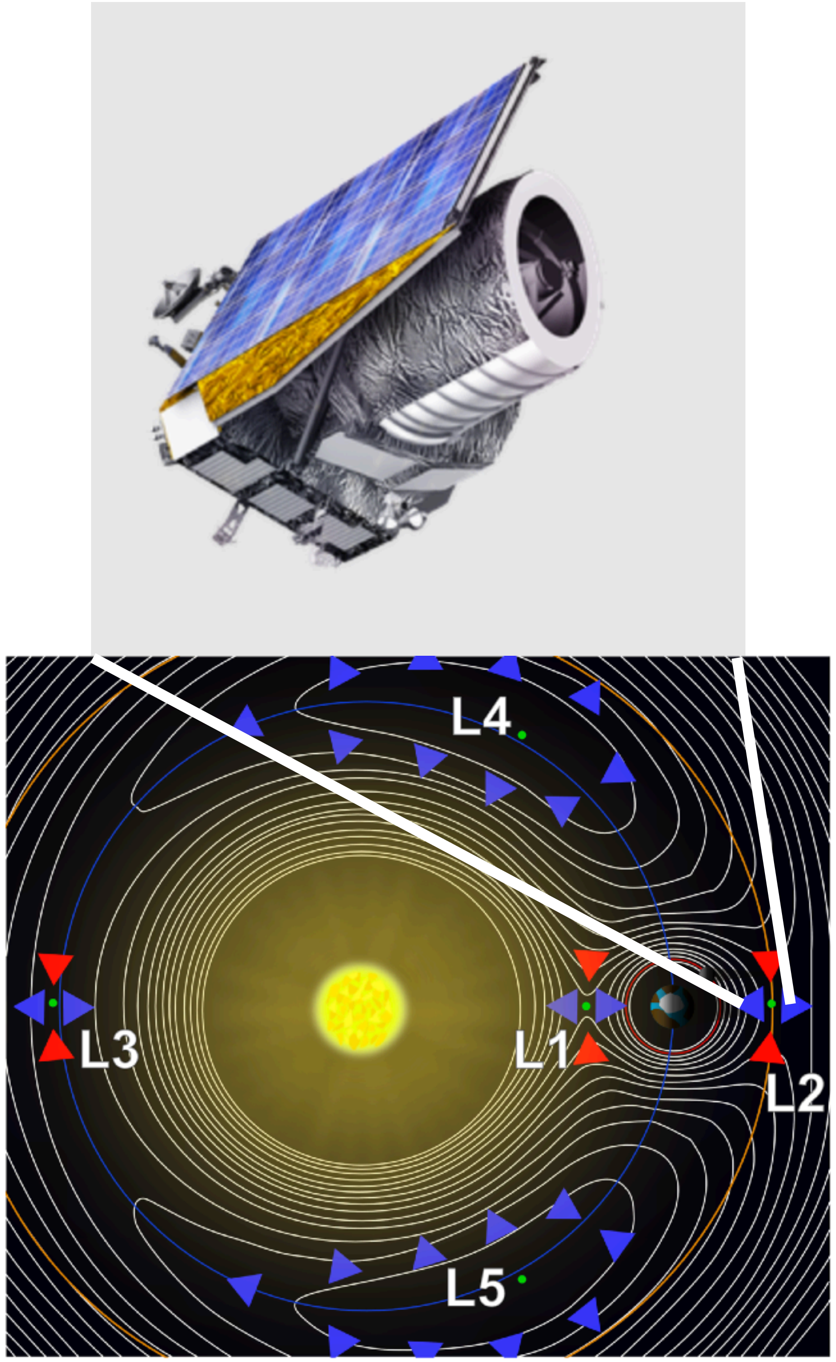

Observation model

Name	Explosion	Progenitor	Mass
R250[a]	PISN	RSG	250 $M_\odot$
R225[a]	PISN	RSG	225 $M_\odot$
R200[a]	PISN	RSG	200 $M_\odot$
R175[a]	PISN	RSG	175 $M_\odot$
R150[a]	PISN	RSG	150 $M_\odot$
He130[a]	PISN	WR	130 $M_\odot$
He120[a]	PISN	WR	120 $M_\odot$
He110[a]	PISN	WR	110 $M_\odot$
He100[a]	PISN	WR	100 $M_\odot$
He090[a]	PISN	WR	90 $M_\odot$
SLSN[b]	SLSN	-	-

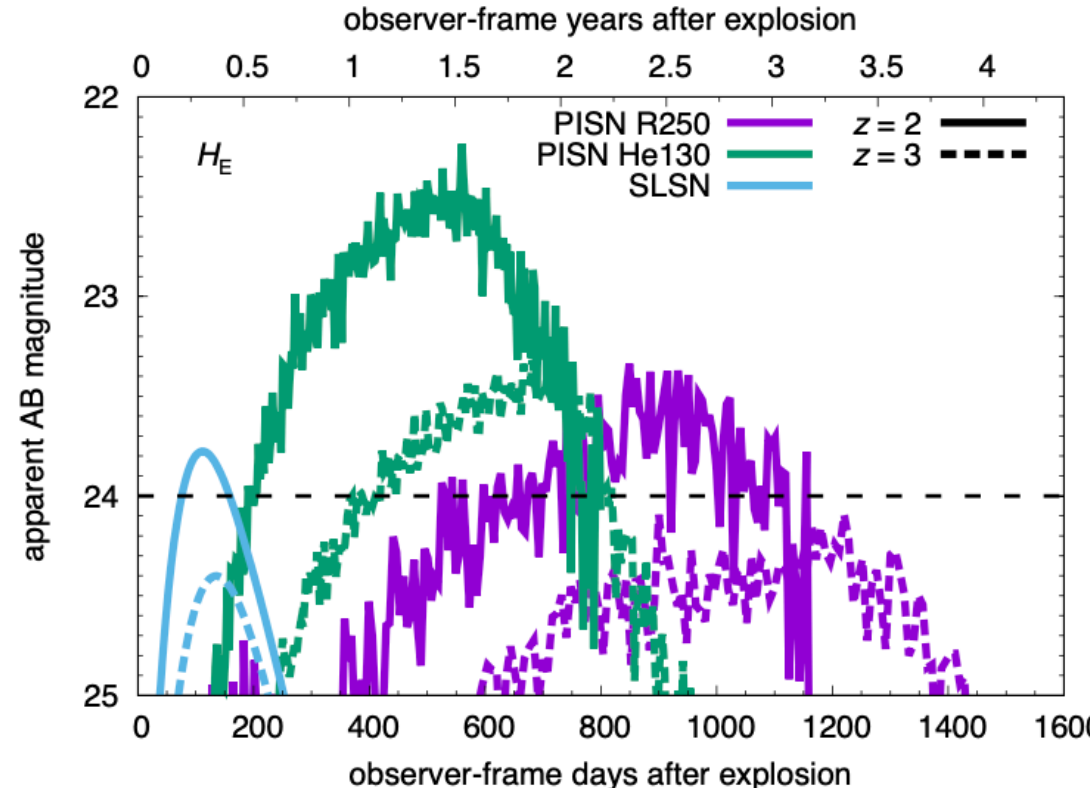

Euclid Deep Fields (EDF)

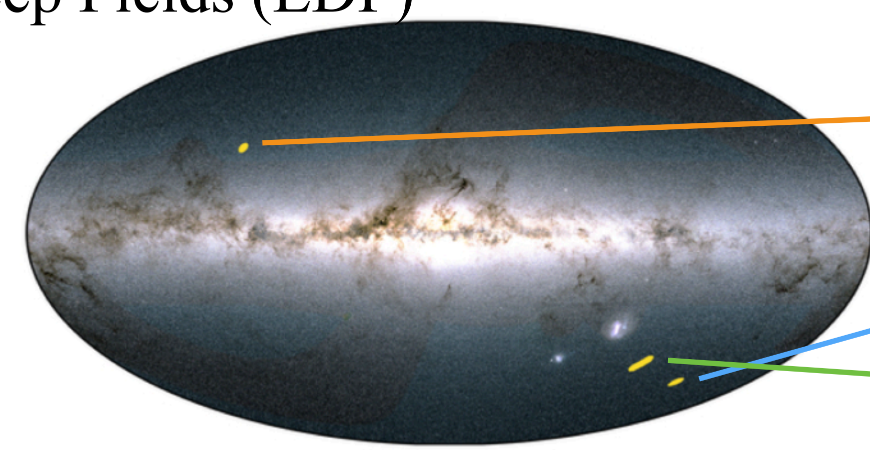

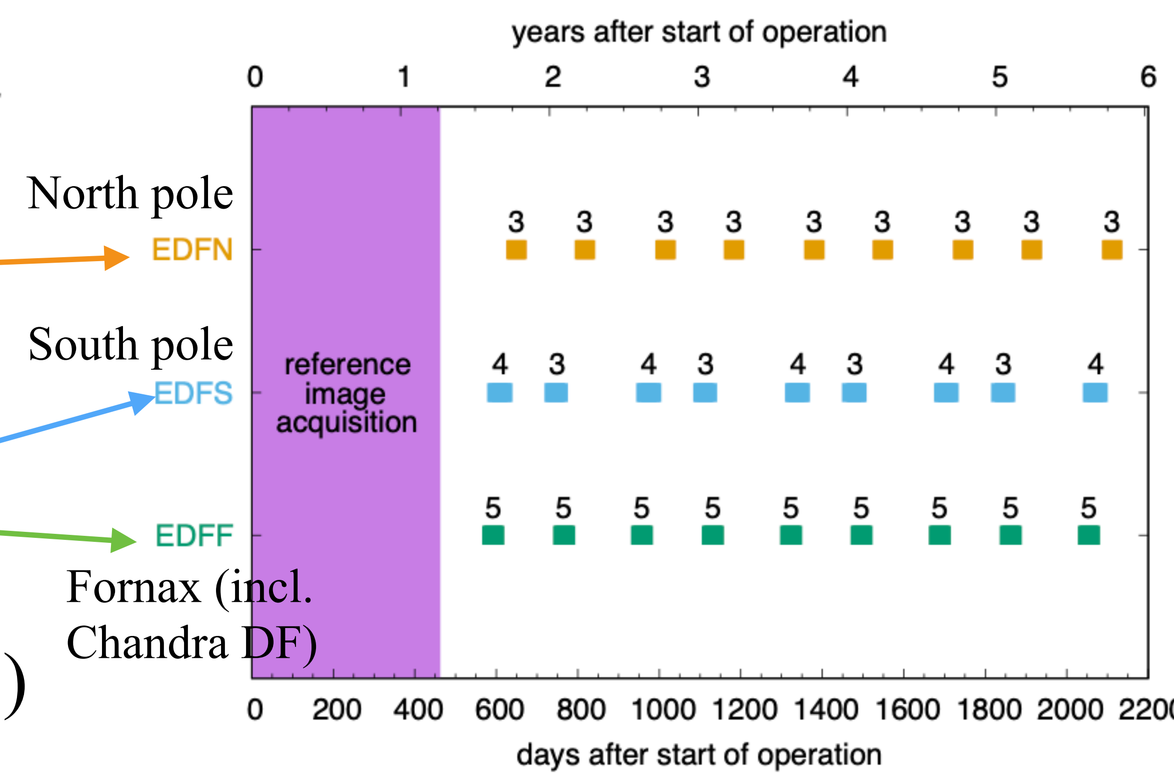

Moriya et al. (2022, arXiv:2204.08727)

PISN detection number

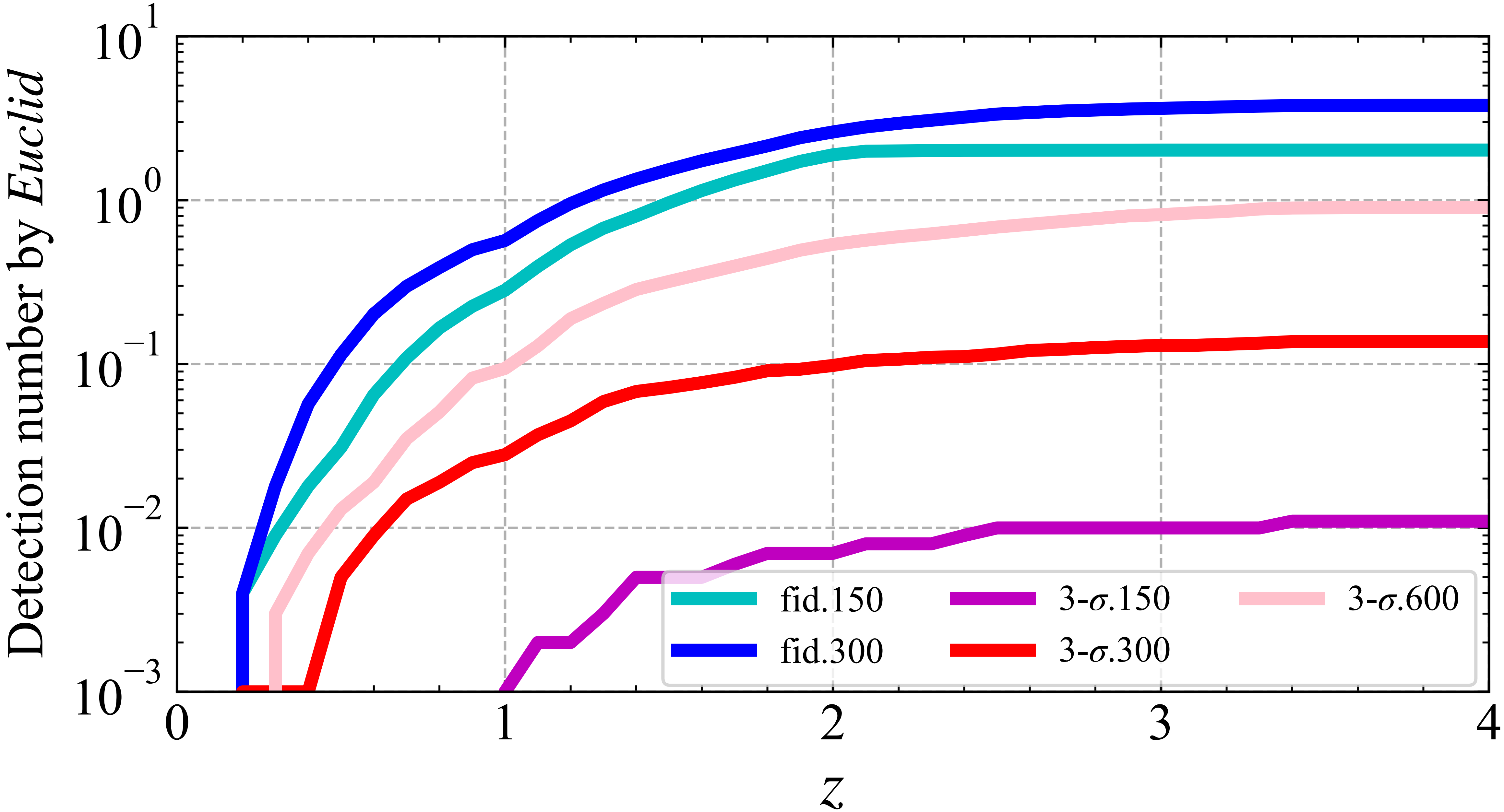

- Few detections → Fiducial PISN model
- No detection → 3-σ PISN model
- 1 detection → Ejecta mass estimate required

Caveats

- PISN observation model is based on the fiducial PISN model.
- There is no PISN model with $M_{\rm c,He} = 180 M_\odot$.
- PISNe with $M_{\rm c,He} > 130 M_\odot$ is assumed to be PISNe with $M_{\rm c,He} = 130 M_\odot$.
- PISNe with $M_{\rm c,He} = 180 M_\odot$ are possibly more bright than with $M_{\rm c,He} = 130 M_\odot$.
- The detection number for 3-σ models may be larger than our estimate.

Takahashi (2018)

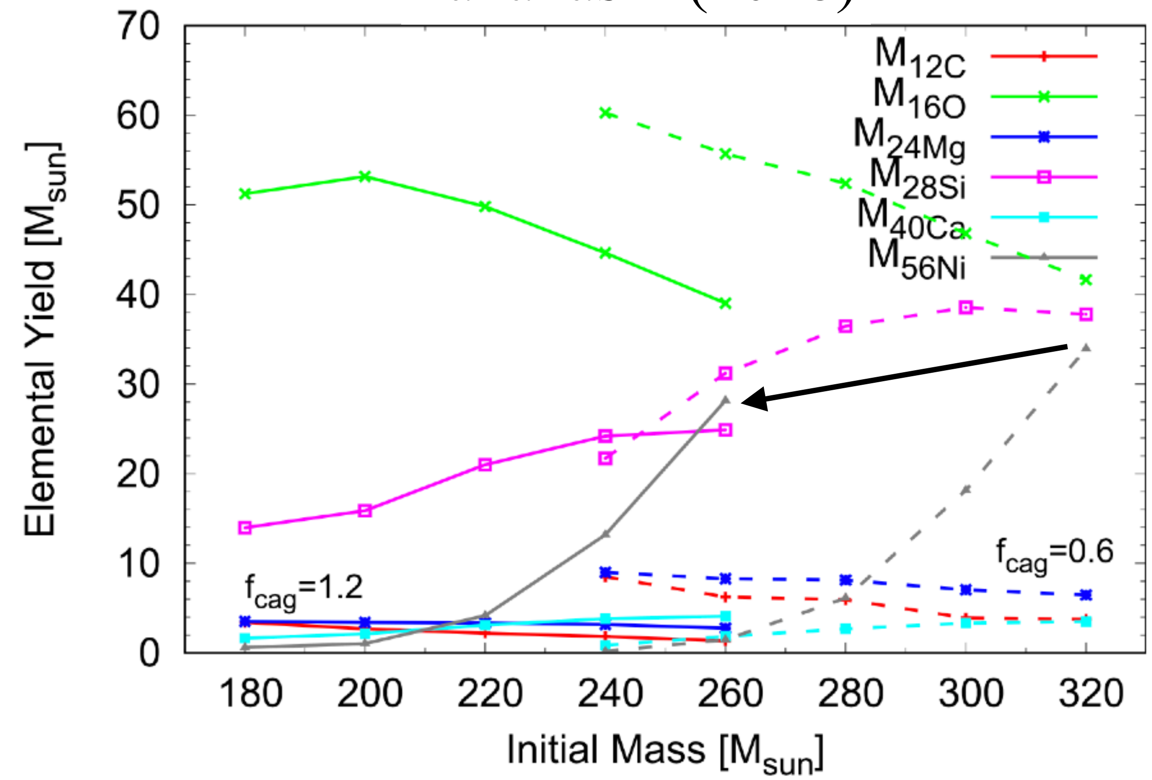

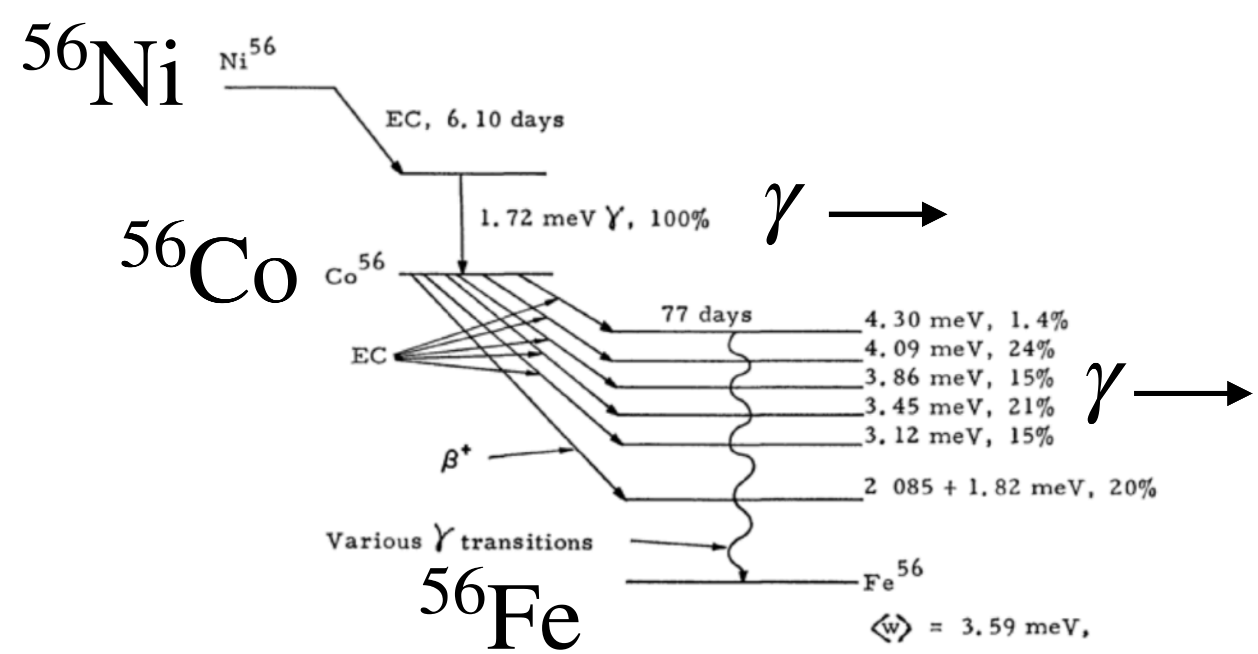

Summary

- The isolated binary scenario for binary BHs is still alive.
- Whichever $^{12}\mathrm{C}(\alpha, \gamma)^{16}\mathrm{O}$ rate we choose.
- The PISN event rate can constrain the $^{12}\mathrm{C}(\alpha, \gamma)^{16}\mathrm{O}$ rate by Euclid survey.
    - Few detections of type I: the fiducial rate
    - No detection: the 3-σ smaller rate
    - One detection of type I: mass estimate definitely required
- We need detail observation models for PISNe with the 3-σ smaller rate.